Computational and Structural Biotechnology Journal 19 (2021) 2990–3005

COMPUTATIONAL AND STRUCTURAL BIOTECHNOLOGY JOURNAL

journal homepage: www.elsevier.com/locate/csbj

Essential requirement of complex number for oscillatory phenomenon in intracellular trafficking process

Yoshinori Marunaka M.D., Ph.D. [a,b,c,1,*], Katsumi Yagi Ph.D. [a,d,1,*]

[a] Medical Research Institute, Kyoto Industrial Health Association, Nakagyo-ku, Kyoto 604-8472, Japan
[b] Research Center for Drug Discovery and Pharmaceutical Development Science, Research Organization of Science and Technology, Ritsumeikan University, Kusatsu 525-8577, Japan
[c] Department of Molecular Cell Physiology, Kyoto Prefectural University of Medicine, Kamigyo-ku, Kyoto 802-8566, Japan
[d] Luis Pasteur Center for Medical Research, Sakyo-ku, Kyoto 606-8225, Japan

ARTICLE INFO

Article history:
Received 24 February 2021
Received in revised form 20 April 2021
Accepted 20 April 2021
Available online 25 April 2021

Keywords:
Mathematical analysis
Complex number
Oscillation
Intracellular trafficking

ABSTRACT

Intracellular protein trafficking processes consisting of three intracellular states are described by three differential equations. To solve the equations, a quadratic equation is required, and its roots are generally real or complex. The purpose of the present study is to clarify the meanings of roots of real and complex numbers. To clarify the point, we define that: 1) 'k_I' is the insertion rate from an insertion state trafficking to the plasma membrane state; 2) 'k_E', the endocytotic rate from the plasma membrane state trafficking to a recycling state; 3) 'k_R', the recycling rate from the recycling state trafficking to the insertion state. Amounts of proteins in three states are expressed as $\alpha e^{lt} + \beta e^{mt} + \gamma$ with α, β, γ = constant and l and m are roots of a quadratic equation, $r^2 + (k_I + k_E + k_R)r + (k_Ik_E + k_Ik_R + k_Ek_R) = 0$. When l and m are real $\left(\left({k_I}^2 + {k_E}^2 + {k_R}^2\right) > 2(k_Ik_E + k_Ek_R + k_Rk_I)\right)$, amounts of proteins in three states shows no oscillatory change but a monotonic change after a transient increase (or decrease); when l and m are complex $\left(\left({k_I}^2 + {k_E}^2 + {k_R}^2\right) < 2(k_Ik_E + k_Ek_R + k_Rk_I)\right)$, amounts of proteins in three states are expressed as $\alpha e^{lt} + \beta e^{mt} + \gamma = 2\sqrt{g^2 + h^2}\sin(bt + \sigma)e^{at} + \gamma$ (α, β, l, m = complex and γ, a, b, g, h, σ = real: α, β = conjugate each other; l, m = conjugate each other), showing an oscillatory change with time. The frequency of oscillatory change appearance is evaluated to be 60% at random combinations of three trafficking rates, k_I, k_E and k_R. The present study indicates that complex numbers have an essentially important meaning in appearance of oscillatory phenomena in bodily and cellular function.

1. Introduction

Epithelial Na^+ channel (ENaC) contributes to determination of the body fluid content through control of the amount of Na^+ reabsorption in the kidney, which is mainly regulated by the amount (number) of ENaC located on the plasma membrane of cortical tubules in the kidney [1–4]. The body fluid content is one of the most important key factors influencing blood pressure [4–10]. Therefore, understandings on molecular mechanisms regulating ENaC amounts on the plasma membrane are essentially required to obtain knowledges on the molecular mechanism controlling blood pressure [5–8]. Here, it is notable that the intracellular trafficking process is one of the key factors determining ENaC amounts on the plasma membrane [5–8]. A study reports the intracellular trafficking process of epithelial Na^+ channel (ENaC), providing quantitative information on the intracellular ENaC trafficking [11]. The quantitative information is very useful to understand the molecular mechanism of the intracellular ENaC trafficking process. Biochemical, immunochemical and molecular biological approaches provide us with quantitative information on the amount of ENaC located on the plasma membrane [3]. However, the time resolution provided by these techniques is not high enough to quantitatively analyze the ENaC trafficking kinetics. On one hand, electrophysiological techniques enable us to detect the amount of transcellular Na^+ transport in renal epithelia via ENaC [4] with a high enough time resolution for determination of the ENaC trafficking kinetics. Unfortunately, electrophysiological

* Corresponding authors at: Medical Research Institute, Kyoto Industrial Health Association, General Incorporated Foundation, 67 Kitatsuboi-cho, Nishino-kyo, Nakagyo-ku, Kyoto 604-8472, Japan.
E-mail addresses: marunaka@koto.kpu-m.ac.jp (Y. Marunaka), ktsmyg@yahoo.co.jp (K. Yagi).
[1] Yoshinori Marunaka and Katsumi Yagi equally contributed to this work.

https://doi.org/10.1016/j.csbj.2021.04.053

techniques alone provide no information on intracellular trafficking processes of ENaC, the kinetics of which is one of the most important key factors regulating the ENaC amount on the plasma membrane of renal epithelia. This means that combination of the mathematical model, electrophysiological and other techniques such as biochemical, immunochemical and molecular biological approaches is a very powerful method to obtain detailed understandings on the regulatory mechanism of ENaC trafficking. Further, the mathematical model can be applied not only for the intracellular ENaC trafficking but also for the intracellular trafficking processes of other proteins such as insulin receptor etc. Therefore, in a general meaning, the mathematical model is very useful for analysis in the intracellular trafficking process of proteins such as insulin receptor and glucose transporter etc. [12–14].

We have reported a mathematical model using differential equations [1,15–17]. In our previous reports [1,15–17], we just considered real numbers as roots for the equation that was required to resolve differential equations showing the intracellular ENaC trafficking process. In these reports [1,15–17], the mathematical model could simulate only two types of phenomena if only real numbers would be considered as roots for the equation; 1) a monotonic increase or decrease with no extremum value, and 2) a transient increase (or decrease) followed by a monotonic decrease (or increase) with only one extremum value. However, oscillatory changes could not be simulated using the mathematical model considering only real numbers as roots for the equation [1,15–17]. We frequently observe biological phenomena showing oscillatory changes essentially required for the maintenance of biological activity; *e.g.*, oscillatory changes are observed in the membrane potentials of pancreatic ß cells [18] and cardiac cells [19], the intracellular Ca^{2+} concentration ($[Ca^{2+}]$) in adipocytes [20], pancreatic α cells [21] and β cells [22], the movement of insulin-containing granules in pancreatic β cells [23], regular rhythms of the brain [24], and delayed electroretinogram potential in diabetic rats [24]. These oscillatory phenomena [18–24] play key roles in homeostasis of body environments. The lack of ability to simulate oscillatory phenomena in the mathematical model using differential equations [1,15–17] would be due to consideration of only real numbers but not complex numbers as roots for the equation required to resolve differential equations showing the intracellular ENaC trafficking process, since we did not consider complex numbers as roots for the equation in the reports [1,15–17]. Therefore, in the present study, to clarify the meaning of complex roots, we applied a simple mathematical model showing three states in cells and tried to explore if oscillatory changes could be simulated by considering complex numbers as roots for the equation even in the simple mathematical model. We here firstly report that: 1) in the case that the equation has two real roots without any 'complex' root, the mathematical model cannot simulate oscillatory changes in the ENaC amount in each state, but only monotonical changes; 2) in the case of two 'complex' roots, it is able to simulate an oscillatory change with the time. Thus, the mathematical model proposed in the present study has ability to simulate both monotonic and oscillatory phenomena observed in the biological activity, and is useful for simulations of various biological phenomena and detailed understandings on molecular mechanisms of protein trafficking.

2. Methods

2.1. Mathematical methods providing a model of intracellular protein trafficking

In the present study, we propose three-state mathematical model shown in Fig. 1: 1) an insertion state where a protein can be trafficked to the plasma membrane with the insertion rate, k_I; 2) a plasma membrane state, at which a protein can show its function as a plasma membrane protein such as an ion channel or a hormonal receptor, and be endocytotically trafficked to a recycling state with the endocytotic rate, k_E; 3) an intracellular recycling state where a protein is trafficked back to the insertion state with the recycling rate, k_R. Here, k_I, k_E and k_R are regulated by various hormones such as aldosterone and insulin [1]. k_E is also regulated by connexin 30 [2]. Further, k_R is regulated by Rab-family small GTPase [3]. The amounts (numbers) of the proteins in the insertion state, the plasma membrane state and the recycling state are respectively represented as *Ins*, *Plas* and *Rec*. $Ins(t)$, $Plas(t)$ and $Rec(t)$ respectively represent the amounts (numbers) of the proteins in the insertion state, the plasma membrane state and the recycling state at time = t, which is the time after application of stimulants affecting any trafficking rate, k_I, k_E or k_R. $Ins(t)$, $Plas(t)$ and $Rec(t)$ are respectively represented by Eqs. (1) through (3).

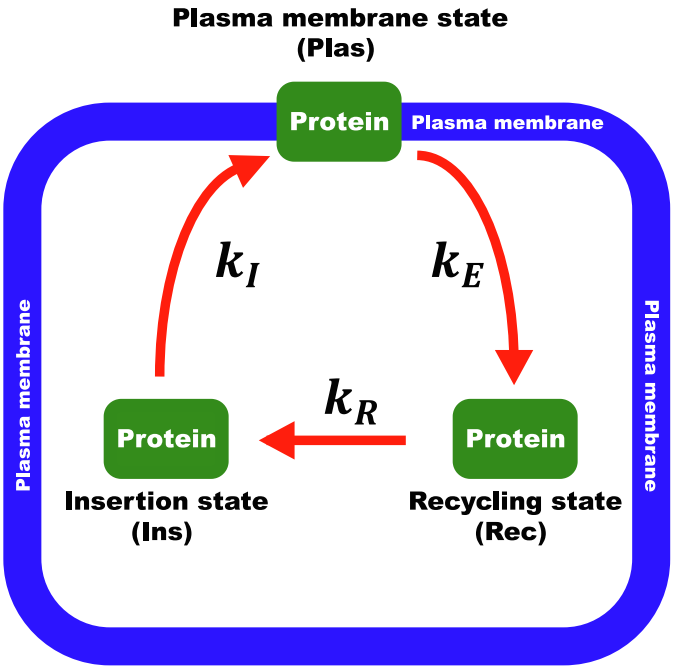

Fig. 1. An intracellular protein trafficking model. 1) An insertion state (*Ins*): this state contains proteins that access the plasma membrane with an insertion rate into the apical membrane (k_I). 2) A plasma membrane state (*Plas*): this state contains proteins in the plasma membrane. 3) A recycling state (*Rec*): this state contains proteins retrieved from the plasma membrane with an endocytotic rate (k_E), and then the protein is trafficked back to the insertion state (Ins) with a recycling rate (k_R). k_I, k_E and k_R are regulated by various hormones such as aldosterone and insulin [1]. k_E is also regulated by connexin 30 [2]. Further, k_R is regulated by Rab-family small GTPase [3].

$$\frac{dIns(t)}{dt} = -k_I Ins(t) + k_R Rec(t) \quad (1)$$

$$\frac{dPlas(t)}{dt} = -k_E Plas(t) + k_I Ins(t) \quad (2)$$

$$\frac{dRec(t)}{dt} = -k_R Rec(t) + k_E Plas(t) \quad (3)$$

where t is the time after application of stimulants affecting any trafficking rate, k_I, k_E or k_R: $Ins(t) \geqq 0$, $Plas(t) \geqq 0$, $Rec(t) \geqq 0$, and $k_I > 0$, $k_E > 0$ and $k_R > 0$. In a trafficking model shown in Fig. 1, we provide a condition that the total amount of proteins in three states is constant, P (*i.e.*, Eq. (1) + Eq. (2) + Eq. (3) $= \frac{dIns(t)}{dt} + \frac{dPlas(t)}{dt} + \frac{dRec(t)}{dt} = 0$).

$$Ins(t) + Plas(t) + Rec(t) = P \tag{4}$$

Eqs. (5), (6) and (7) respectively represent solutions of $Ins(t)$, $Plas(t)$ and $Rec(t)$ described by Eqs. (1), (2) and (3) (see Eq. (*A*1) through (*A*38), Eq. (*AM*1) through (*AM*3), and Eq. (*AM*47) through (*AM*63) described in 'Appendix' for detailed processes to obtain Eqs. (5), (6) and (7).

$$Ins(t) = C_1\left(\frac{k_E + l}{k_I}\right)e^{lt} + C_2\left(\frac{k_E + m}{k_I}\right)e^{mt} + C_3\frac{k_E}{k_I} \tag{5}$$

$$Plas(t) = C_1 e^{lt} + C_2 e^{mt} + C_3 \tag{6}$$

$$Rec(t) = C_1\frac{(k_I + l)(k_E + l)}{k_R k_I}e^{lt} + C_2\frac{(k_I + m)(k_E + m)}{k_R k_I}e^{mt} + C_3\frac{k_E}{k_R} \tag{7}$$

In Eqs. (5), (6) and (7), C_1, C_2 and C_3 are constant: C_1, C_2 and C_3 are respectively represented by Eqs. (8), (9) and (10), and l and m are roots of Eq. (11) (defined as $l < m$).

$$C_1 = -\frac{1}{l(l-m)}[k_I(k_I + k_E + m)Ins(0) - (k_E + m)k_E Plas(0) - k_R k_I Rec(0)] \tag{8}$$

$$C_2 = \frac{1}{m(l-m)}[k_I(k_I + k_E + l)Ins(0) - k_E(k_E + l)Plas(0) - k_R k_I Rec(0)] \tag{9}$$

$$C_3 = -\frac{1}{lm}[k_I(k_I + k_E + l + m)Ins(0) - (k_E + l)(k_E + m)Plas(0) - k_R k_I Rec(0)] \tag{10}$$

$$\lambda^2 + (k_I + k_E + k_R)\lambda + (k_I k_E + k_E k_R + k_R k_I)$$

$$= (\lambda - l)(\lambda - m)$$

$$= \lambda^2 - (l + m)\lambda + lm = 0 \tag{11}$$

where $Ins(0)$, $Plas(0)$ and $Rec(0)$ are respectively $Ins(t)$, $Plas(t)$ and $Rec(t)$ at $t = 0$. Eqs. (12) and (13) are obtained from Eq. (11), since $k_I > 0$, $k_E > 0$ and $k_R > 0$.

$$l + m = -(k_I + k_E + k_R) < 0 \tag{12}$$

$$lm = k_I k_E + k_E k_R + k_R k_I > 0 \tag{13}$$

The discriminant of Eq. (11) is as follows.

$$D = (k_I + k_E + k_R)^2 - 4(k_I k_E + k_E k_R + k_R k_I)$$
$$= {k_I}^2 + {k_E}^2 + {k_R}^2 - 2(k_I k_E + k_E k_R + k_R k_I) \tag{14}$$

3. Results

3.1. Time-dependent change of protein amount in each state when **l** and **m** are real numbers (**D** > 0)

From Eqs. (12) and (13), we obtain Eqs. (15) and (16).

$$l < 0 \tag{15}$$

$$m < 0 \tag{16}$$

$Ins(t)$, $Plas(t)$ and $Rec(t)$ (see Eqs. (5), (6) and (7)) can be generally expressed as $\varphi(t)$ shown as Eq. (17).

$$\varphi(t) = \alpha e^{lt} + \beta e^{mt} + \gamma \tag{17}$$

where l, m, α, β and γ are real numbers. The time-dependent changes of $Ins(t)$, $Plas(t)$ and $Rec(t)$ are generally expressed as Eq. (18).

$$\frac{d\varphi(t)}{dt} = l\alpha e^{lt} + m\beta e^{mt} = m\beta e^{lt}\left(\frac{l\alpha}{m\beta} + e^{(m-l)t}\right) \tag{18}$$

We define t_e as t at which $\varphi(t)$ shows its extremum value: *i.e.*, $\frac{d\varphi(t)}{dt} = 0$ at t_e (see Eq. (19)).

$$t_e = \frac{1}{m-l}\ln\left(-\frac{l\alpha}{m\beta}\right) \tag{19}$$

Since l, m, α and β are constant, t_e determined by Eq. (19) is at most one for each equation $Ins(t)$, $Plas(t)$ or $Rec(t)$. Therefore, each solution of $Ins(t)$, $Plas(t)$ or $Rec(t)$ has at most one extremal value: *i.e.* 1) when the signs of α and β are different, $Ins(t)$, $Plas(t)$ or $Rec(t)$ respectively shows a monotonic increase (or decrease) after a transient decrease (or increase), converging to $C_3\frac{k_E}{k_I}$, C_3 or $C_3\frac{k_E}{k_R}$ (see Eq. (5) through (11)); 2) when the signs of α and β are same, $Ins(t)$, $Plas(t)$ or $Rec(t)$ respectively shows a monotonic increase (or decrease) without any extremal value, converging to $C_3\frac{k_E}{k_I}$, C_3 or $C_3\frac{k_E}{k_R}$ (see Eqs. (5) through (11)).

3.2. The time-dependent changes of protein amounts in **Ins**(**t**), **Plas**(**t**) and **Rec**(**t**) in a case of D > 0 with $\boldsymbol{k_I}$ = 1.0 h^{-1}, $\boldsymbol{k_E}$ = 0.4 h^{-1}, $\boldsymbol{k_R}$ = 0.1 h^{-1} (D = 0.09): **Ins**(0) = 1, **Plas**(0) = 0 and **Rec**(0) = 0

Fig. 2A shows the time-dependent changes of protein amounts staying at *Ins*, *Plas* and *Rec* in a case with $k_I = 1.0\ h^{-1}$, $k_E = 0.4\ h^{-1}$, $k_R = 0.1\ h^{-1}$ ($D = 0.09$), $Ins(0) = 1$, $Plas(0) = 0$ and $Rec(0) = 0$. In this case, $Ins(t)$ decreases and reaches the minimal value at 4.6 h (Blue line in Fig. 2A; also see Fig. 2B and C). After reaching its minimal value at 4.6 h, $Ins(t)$ monotonically increases, converging to $C_3\frac{k_E}{k_I}$ (=0.074: see Eq. (5): Blue line in Fig. 2A; also see Fig. 2B and C). $Plas(t)$ increases and reaches the maximal value at 1.6 h (Red line in Fig. 2A: also see Fig. 2B and C). After reaching its maximal value, $Plas(t)$ monotonically decreases, converging to C_3 (=0.185: see Eq. (6): Red line in Fig. 2A: also see Fig. 2B and C). $Rec(t)$ monotonically increases, converging to $C_3\frac{k_E}{k_R}$ (=0.741; see Eq. (7)) without any maximal value (Green line in Fig. 2A: also see Fig. 2B and C). However, the detailed time-dependent change in $Ins(t)$, $Plas(t)$ or $Rec(t)$ is not clearly seen in Fig. 2A. Therefore, as the first step for clear recognition of the time-dependent changes in the values of $Ins(t)$, $Plas(t)$ and $Rec(t)$ described above, each converging value (C_3k_E/k_I, C_3, or C_3k_E/k_R) is respectively subtracted from $Ins(t)$, $Plas(t)$ or $Rec(t)$: *i.e.*, all values of $Ins(t) - C_3k_E/k_I$, $Plas(t) - C_3$ and $Rec(t) - k_E/k_R$ converging to 0 (Fig. 2B). As the next step to more clearly show the detailed profiles of the time-dependent changes in $Ins(t) - C_3k_E/k_I$, $Plas(t) - C_3$ and $Rec(t) - k_E/k_R$ described above, we magnify the axis of protein amounts to various levels (see the magnified level of the axis shown above each panel in Fig. 2C): *i.e.*, 1) $Ins(t) - C_3k_E/k_I$ decreases toward its minimal value appearing at 4.6 h, and then monotonically increases, converging to 0 (Blue line in Fig. 2C); $Plas(t) - C_3$ increases toward its maximal value appearing at 1.6 h, and then monotonically decreases, converging to 0 (Red line in Fig. 2C); $Rec(t) - k_E/k_R$ monotonically increases, converging to 0 without any maximal value (Green line in Fig. 2C).

3.3. Time-dependent change of protein amount in each state when l and m are complex (**D** < 0)

When $D < 0$, $Ins(t)$, $Plas(t)$ and $Rec(t)$ shown as Eq. (17) can be generally expressed as $\varphi(t)$ with conditions that l and m = conjugate complex numbers, and α and β = conjugate complex numbers (see Eq. (20), (21), (22) and (23): *c.f.*, Eqs. (*A*85) through (*A*94): α and β respectively correspond to $C_1\left(\frac{k_E+l}{k_I}\right)$ and $C_2\left(\frac{k_E+m}{k_I}\right)$ in $Ins(t)$ (Eq. (5)),

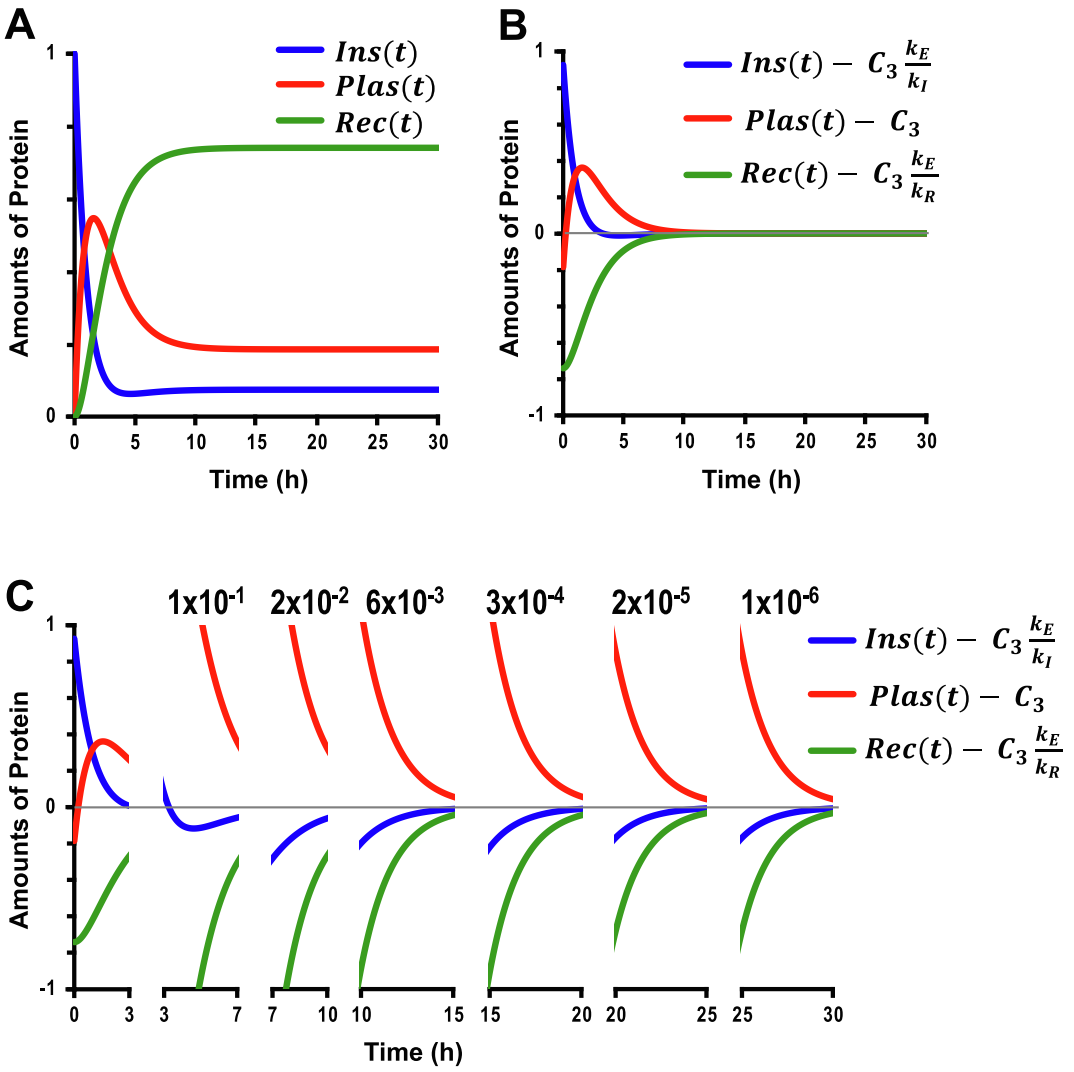

Fig. 2. The time-dependent change of protein amounts staying at *Ins*, *Plas* and *Rec* under the condition with $k_I = 1.0\ h^{-1}$, $k_E = 0.4\ h^{-1}$, $k_R = 0.1\ h^{-1}$ ($D = 0.09$), $Ins(0) = 1$, $Plas(0) = 0$ and $Rec(0) = 0$. A) The time-dependent change of $Ins(t)$, $Plas(t)$ and $Rec(t)$ with the axis of protein amounts from 0 to 1. $Ins(t)$ decreases toward its minimal value appearing at 4.6 h, and then monotonically increases, converging to C_3k_E/k_I (Blue line). $Plas(t)$ increases toward its maximal value appearing at 1.6 h, and then monotonically decreases, converging to C_3 (Red line). $Rec(t)$ monotonically increases, converging to C_3k_E/k_R without any maximal value (Green line). B) The time-dependent changes in $Ins(t) - C_3k_E/k_I$ (Red line), $Plas(t) - C_3$ (Blue line) and $Rec(t) - C_3k_E/k_R$ (Green line) converging to 0. C) The detailed profiles of $Ins(t) - C_3k_E/k_I$ (Blue line), $Plas(t) - C_3$ (Red line) and $Rec(t) - C_3k_E/k_R$ (Green line) with magnified axes of protein amounts to various level. The value described above each panel shows the magnified level of the protein amount axis.

C_1 and C_2 in $Plas(t)$ (Eq. (6)), and $C_1\frac{(k_I+l)(k_E+l)}{k_Rk_I}$ and $C_2\frac{(k_I+m)(k_E+m)}{k_Rk_I}$ in $Rec(t)$ (Eq. (7)).

$$l = a - ib \tag{20}$$

$$m = a + ib \tag{21}$$

$$\alpha = g + ih \tag{22}$$

$$\beta = g - ih \tag{23}$$

where a, b, g and h are real numbers. Using Eqs. (20), (21), (22) and (23), and 'Euler's formula' with Maclaurin expansion ($e^{i\theta} = \cos\theta + i\sin\theta$), Eq. (17) can be expressed as Eq. (24).

$$\begin{aligned}\varphi(t) &= \alpha e^{lt} + \beta e^{mt} + \gamma = (g+ih)e^{(a-ib)t} + (g-ih)e^{(a+ib)t} + \gamma \\ &= 2(g\cos bt + h\sin bt)e^{at} + \gamma\end{aligned} \tag{24}$$

Here, we define as follows.

$$\cos\sigma = \frac{h}{\sqrt{g^2+h^2}} \tag{25}$$

$$\sin\sigma = \frac{g}{\sqrt{g^2+h^2}} \tag{26}$$

Eq. (24) can be converted to Eq. (27) using 'Trigonometric Addition Formulas' ($\sin\varepsilon\cos\omega + \cos\varepsilon\sin\omega = \sin(\varepsilon+\omega)$) with Eqs. (25) and (26).

$$\varphi(t) = 2(g\cos bt + h\sin bt)e^{at} + \gamma = 2\sqrt{g^2+h^2}\sin(bt+\sigma)e^{at} + \gamma \tag{27}$$

We further define μ as follows (Eqs. (28) and (29)).

$$\cos\mu = \frac{a}{\sqrt{a^2+b^2}} \tag{28}$$

$$\sin\mu = \frac{b}{\sqrt{a^2+b^2}} \tag{29}$$

$\frac{\varphi(t)}{dt}$ is expressed as Eq. (30) using Eqs. (27), (28) and (29), and 'Trigonometric addition formula'($\sin\varepsilon\cos\omega + \cos\varepsilon\sin\omega = \sin(\varepsilon+\omega)$).

$$\frac{d\varphi(t)}{dt} = \frac{d\left(2\sqrt{g^2+h^2}\sin(bt+\sigma)e^{at}+\gamma\right)}{dt}$$
$$= 2\sqrt{g^2+h^2}\sqrt{a^2+b^2}\sin(bt+\sigma+\mu)e^{at} \quad (30)$$

Thus, $\frac{d\varphi(t)}{dt}$ (Eq. (30)) cyclically shows its value = 0 twice with a period cycle of $\frac{2\pi}{b}$: *i.e.*, $\varphi(t)$ has one maximal value and one minimal value cyclically in one period cycle of $\frac{2\pi}{b}$. Eq. (31) is obtained from Eqs. (12), (20) and (21)), and Eq. (32) is obtained from Eqs. (12), (13), (20) and (21)).

$$a = \frac{l+m}{2} = -\frac{k_I+k_E+k_R}{2} < 0 \quad (31)$$

$$b = \frac{\sqrt{4(k_Ik_E+k_Ek_R+k_Rk_I)-(k_I+k_E+k_R)^2}}{2} \quad (32)$$

Since $a < 0$ (see Eq. (31)), $\varphi(t)$ (Eq. (27)) converges to γ in an oscillatory manner with one cyclus of $\frac{2\pi}{b}$. Based on this finding, $Ins(t)$, $Plas(t)$ or $Rec(t)$ respectively converges to $C_3\frac{k_E}{k_I}$, C_3 or $C_3\frac{k_E}{k_R}$ (see Eqs. (5) through (7)) in a time-dependently oscillatory manner with the same cyclus of $\frac{2\pi}{b}$.

3.4. The time-dependent changes of protein amounts in ***Ins***(***t***), ***Plas***(***t***) and ***Rec***(***t***) in a case of $D < 0$ with k_I=1.0 h^{-1}, k_E=0.8 h^{-1}, k_R=0.5 h^{-1} (***D***=-1.51): ***Ins***(0) = 1, ***Plas***(0) = 0 and ***Rec***(0) = 0

We show the time-dependent changes of protein amounts staying at *Ins*, *Plas* and *Rec* in a case with k_I=1.0 h^{-1}, k_E=0.8 h^{-1}, k_R=0.5 h^{-1} (D=-1.51): $Ins(0) = 1$, $Plas(0) = 0$ and $Rec(0) = 0$ in Fig. 3A. In this case, $Ins(t)$ shows oscillatory changes in time-dependent manners, converging to C_3k_E/k_I (=0.235) shown in Eq. (5) (see blue lines in Fig. 3A). $Plas(t)$ also shows oscillatory changes in time-dependent manners, converging to C_3 (=0.294) shown in Eq. (6) (see red lines in Fig. 3A). Similarly, $Rec(t)$ shows oscillatory changes in time-dependent manners, converging to C_3k_E/k_R (=0.471) shown in Eq. (7) (see green lines in Fig. 3A). However, the oscillatory changes of $Ins(t)$, $Plas(t)$ or $Rec(t)$ are not clearly recognized in Fig. 3A. Therefore, as the first step for clear recognition of the oscillatory changes in $Ins(t)$, $Plas(t)$ and $Rec(t)$ against time

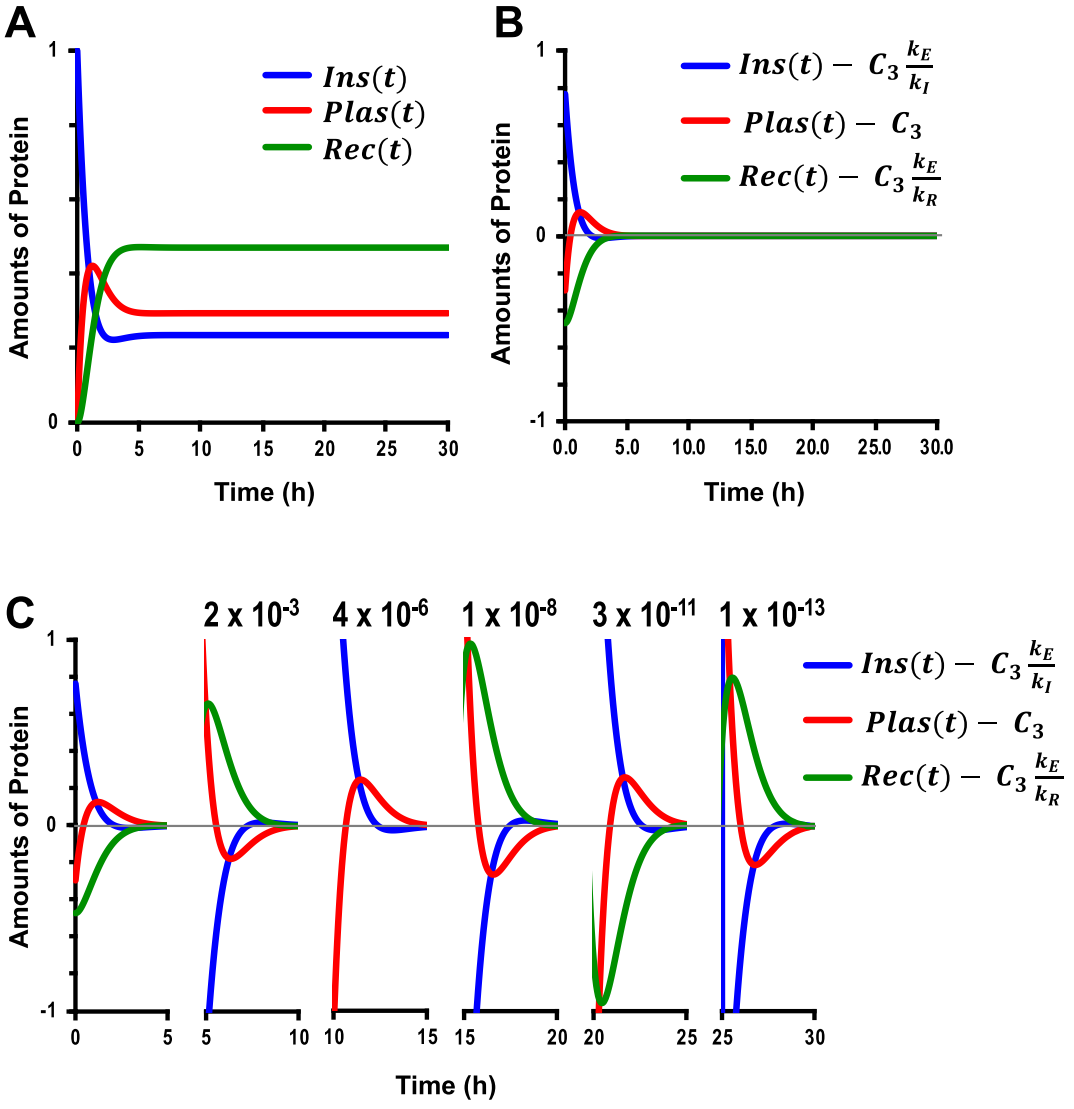

Fig. 3. The time-dependent changes of protein amounts under the condition with k_I=1.0 h^{-1}, k_E=0.8 h^{-1}, k_R=0.5 h^{-1} (D=-1.51): $Ins(0) = 1$, $Plas(0) = 0$ and $Rec(0) = 0$. A) $Ins(t)$ shows time-dependently oscillatory changes, converging to C_3k_E/k_I (Blue line). $Plas(t)$ also shows time-dependently oscillatory changes, converging to C_3 (Red line). Similarly, $Rec(t)$ shows time-dependently oscillatory changes, converging to C_3k_E/k_R (Green line). B) The time-dependent changes in $Ins(t) - C_3k_E/k_I$ (Red line), $Plas(t) - C_3$ (Blue line) and $Rec(t) - C_3k_E/k_R$ (Green line) converging to 0. C) The detailed profiles of $Ins(t) - C_3k_E/k_I$ (Blue line), $Plas(t) - C_3$ (Red line) and $Rec(t) - C_3k_E/k_R$ (Green line) with magnified axes of protein amounts to various levels. The value described above each panel shows the magnified level of the protein amount axis.

(t), each converging value (C_3k_E/k_I, C_3, or C_3k_E/k_R) is respectively subtracted from $Ins(t)$, $Plas(t)$ or $Rec(t)$: *i.e.*, all values of $Ins(t) - C_3k_E/k_I$ (Blue line), $Plas(t) - C_3$ (Red line) and $Rec(t) - C_3k_E/k_R$ (Green line) converge to 0 (Fig. 3B). As the next step to more clearly show the oscillatory changes of $Ins(t) - C_3k_E/k_I$, $Plas(t) - C_3$ and $Rec(t) - C_3k_E/k_R$ in time-dependent manners, we magnify the axis of protein amounts to various levels (Fig. 3C; the magnified level of axis is shown above each panel of Fig. 3C). The time-dependent oscillations in the values of $Ins(t) - C_3k_E/k_I$ (Blue line), $Plas(t) - C_3$ (Red line) and $Rec(t) - C_3k_E/k_R$ (Green line) are clearly seen in Fig. 3C.

3.5. Frequency of l and m being complex numbers

We next try to calculate frequency of l and m being complex numbers when k_I, k_E and k_R are randomly selected. When the value of the discriminant, D (Eq. (14)), is negative ($D < 0$), l and m are complex numbers. This means that $Ins(t)$, $Plas(t)$ or $Rec(t)$ respectively show oscillatory changes with time, t. Therefore, we calculate frequency of $D < 0$ when the values of three trafficking rates, k_I, k_E and k_R, are randomly selected.

We define that three trafficking rates, k_I, k_E or k_R, respectively indicate a position on the axes, X, Y and Z. Under this condition, we should consider three axes X, Y and Z with areas, $X \geqq 0$, $Y \geqq 0$ and $Z \geqq 0$, since all values of k_I, k_E and $k_R \geqq 0$. Here, in the space consisting of axes X, Y and Z with areas $X \geqq 0$, $Y \geqq 0$ and $Z \geqq 0$, we consider a plane, P, containing three points, $(p, 0, 0)$, $(0, p, 0)$ and $(0, 0, p)$: p is a real number ($p > 0$). The plane, P, forms an equilateral triangle with the length of each side = $\sqrt{2}p$ (see Fig. 4) and the center of the equilateral triangle (the plane P) is a point, $(\frac{p}{3}, \frac{p}{3}, \frac{p}{3})$. We next consider a case that a point, (k_I, k_E, k_R), exists on the plane P, indicating that Eq. (33) must function.

$$k_I + k_E + k_R = p \tag{33}$$

Here, Eqs. (34) and (35) are obtained from the discriminant, D (Eq. (14))

$$k_Ik_E + k_Ek_R + k_Rk_I = \frac{(k_I + k_E + k_R)^2 - D}{4} \tag{34}$$

$$k_I{}^2 + k_E{}^2 + k_R{}^2 = D + 2(k_Ik_E + k_Ek_R + k_Rk_I) \tag{35}$$

Thus,

$$k_I{}^2 + k_E{}^2 + k_R{}^2 = \frac{(k_I + k_E + k_R)^2 + D}{2} \tag{36}$$

Therefore, Eq. (37) is obtained from Eqs. (33) and (36).

$$k_I{}^2 + k_E{}^2 + k_R{}^2 = \frac{p^2 + D}{2} \tag{37}$$

On the other hand, using Eqs. (33) and (37) the distance, d, between two points, (k_I, k_E, k_R) and $(\frac{p}{3}, \frac{p}{3}, \frac{p}{3})$, the center of the plane P, is expressed in Eqs. (38) and (39).

$$d^2 = \left(k_I - \frac{p}{3}\right)^2 + \left(k_E - \frac{p}{3}\right)^2 + \left(k_R - \frac{p}{3}\right)^2 = \frac{p^2}{6} + \frac{D}{2} \tag{38}$$

$$d = \sqrt{\frac{p^2}{6} + \frac{D}{2}} = \sqrt{\frac{p^2}{6}\left(1 + \frac{6}{p^2}\frac{D}{2}\right)} = \frac{p}{\sqrt{6}}\sqrt{1 + \frac{3D}{p^2}} \tag{39}$$

When $D > 0$, $d > \frac{p}{\sqrt{6}}$ (40)

When $D < 0$, $d < \frac{p}{\sqrt{6}}$ (41)

Since the plane P is an equilateral triangle of each side = $\sqrt{2}p$, the radius, R, of the circle inscribing the equilateral triangle of the plane P is $\frac{p}{\sqrt{6}}$ (see Fig. 4), and the center of the circle is $(\frac{p}{3}, \frac{p}{3}, \frac{p}{3})$, which is same as that of the equilateral triangle of

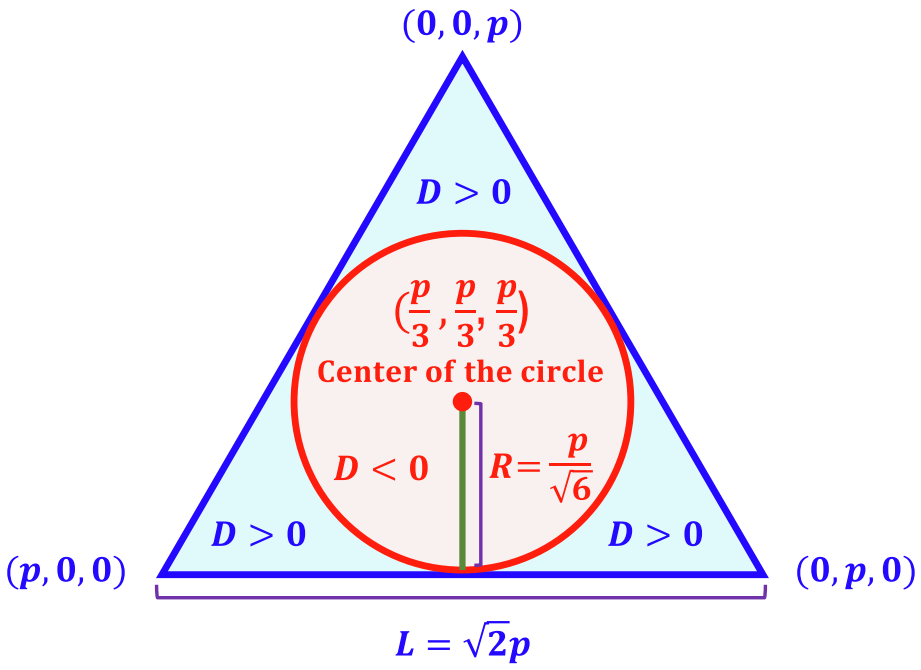

Fig. 4. The relationship between the plane, P, an equilateral triangle described by blue lines and the circle described by a red line inscribing the equilateral triangle of the plane, P. Three axes X, Y and Z with areas $X \geqq 0$, $Y \geqq 0$ and $Z \geqq 0$. We define that three trafficking rates, k_I, k_E and k_R, respectively indicate the position on the axes, X, Y and Z. Here, in the space consisting of axes X, Y and Z with areas $X \geqq 0$, $Y \geqq 0$ and $Z \geqq 0$, we consider a plane, P, containing three points, $(p, 0, 0)$, $(0, p, 0)$ and $(0, 0, p)$: p is a real number ($p > 0$). The plane, P, is determined by three points $(p, 0, 0)$, $(0, p, 0)$ and $(0, 0, p)$ (p = a real number ($p > 0$) with each side = $\sqrt{2}p$ and the center of the equilateral triangle (the plane P) is a point, $(p/3, p/3, p/3)$. Since the plane, P, is an equilateral triangle of each side = $\sqrt{2}p$, the radius, R, of the circle inscribing the equilateral triangle of the plane P is $p/\sqrt{6}$, and the center of the circle is $(p/3, p/3, p/3)$, which is same as that of the equilateral triangle of the plane P. The area at D>0 (Eq. (14)) is shown by blue, while the area D<0 (Eq. (14)) is shown by red.

the plane P. Therefore, we can obtain the relationships of the equilateral triangle of the plane P and the circle inscribing the equilateral triangle of the plane P and shown in Fig. 4.

When $D > 0$ under a condition with $k_I + k_E + k_R = p$, a point (k_I, k_E, k_R) exists outside the circle inscribing the equilateral triangle, the plane P, since the distance (d) between two points, (k_I, k_E, k_R) and $(\frac{p}{3}, \frac{p}{3}, \frac{p}{3})$, the center of the circle inscribing the equilateral triangle of the plane P is larger than the radius of the inscribing circle (see Eq. (40)).

When $D < 0$ under a condition with $k_I + k_E + k_R = p$, a point (k_I, k_E, k_R) exists inside the circle inscribing the equilateral triangle, the plane P, since the distance (d) between two points, (k_I, k_E, k_R) and $(\frac{p}{3}, \frac{p}{3}, \frac{p}{3})$, the center of the circle inscribing the equilateral triangle of the plane P is smaller than the radius of the inscribing circle (see Eq. (41)). We calculated the ratio of the area inside of the inscribing circle to that of the equilateral triangle, $R_{C/T}$, which is shown as follows.

$$R_{C/T} = \frac{\pi}{3\sqrt{3}} \tag{42}$$

$R_{C/T}$ is about 0.60. This means that the frequency of oscillation occurrence in the amount of protein in each state is about 60% with random combinations of three trafficking rates, k_I, k_E and k_R. Thus, it is not rare but rather predominant that the amount of protein in each state shows an oscillatory change.

4. Discussion

The present study deals with an intracellular trafficking process of protein using a mathematical simulation with differential equations. A quadratic Eq. (11) is used to dissolve differential Eqs. (1), (2) and (3). In a case that quadratic Eq. (11) has two real roots, the protein in an intracellular state shows no oscillatory change but a monotonic decrease (or increase) after a transient increase (or decrease) or a monotonic decrease (or increase) without any extreme value, converging to each eigenvalue determined by k_I, k_E and k_R. On one hand, in a case that a quadratic equation has two complex roots, the protein in an intracellular state converges to each eigenvalue determined by k_I, k_E and k_R with showing an oscillatory change. In both cases, $Ins(t)$, $Plas(t)$ and $Rec(t)$ respectively converge to $C_3 k_E/k_I$, C_3 and $C_3 k_E/k_R$ (see Eq. (10) regarding C_3).

Intracellular protein trafficking plays an important role in physiological function in our body. For example, insulin receptor in an intracellular state is trafficked to the plasma membrane. The insulin receptor is internalized by insulin biding to the receptor. Then, the insulin-bound receptor is dissociated into the receptor and insulin in an intracellular state, in which some receptors are trafficked to the plasma membrane [12–14,25,26]. Most of reports studying recycling processes have applied molecular biological, biochemical and immunochemical techniques to determine the localization of receptors in the intracellular space, providing molecular mechanisms and processes of receptor recycling in detail. Since the time resolution of these techniques is not so high, it is generally difficult to detect time-dependent oscillatory changes in the amounts of proteins including receptors in intracellular states with a high time resolution. The electrophysiological and imaging techniques have advantages with a high time resolution, thus the technique provides us with phenomena showing oscillatory changes in: the membrane potentials of cardiac cells [19] and pancreatic beta cells [18]; intracellular Ca^{2+} concentration in pancreatic alpha cells [21], beta cells [22], and adipocytes [20]; movements of granules including insulin in pancreatic beta cells [23]; regular rhythms of the brain [24]; delayed electroretinogram potential in diabetic rats [24]; ciliary beat frequently [27,28]. However, we have little information on the quantitative change in protein amounts in the intracellular state.

Dee and Shuler [29] have proposed a mathematical model of virus trafficking into the intracellular space and intracellular movement with four major steps (1, a binding process of virus to the receptor forming a virus-receptor coupling complex; 2, internalization process of the complex into endosome; 3, a receptor recycling process; 4) a moving process of virus to nucleus), using linear differential equations. In this study [29], the amount of virus in endosome show a transient increase followed by a decrease with time similar to the result shown in the present study in a case of the discriminant of Eq. (11) having real roots ($D > 0$ in Eq. (14)), and the amount of virus in endosome is described by a couple of exponential equations similar to the result shown in the present study in a case of the discriminant of Eq. (11) having real roots ($D > 0$ in Eq. (14)). This mathematical model [29] proposes a linear, irreversible process except the reversible binding process of virus to the receptor forming a virus-receptor coupling complex before internalization. However, this report [29] proposes no recycling process after internalization of receptors. The recycling process after internalization of proteins including receptors is one of the most important functions maintaining various cellular activities [25,26], leading us to an idea that a mathematical model including recycle processes should be proposed. Thus, the present study proposes a mathematical model including recycling processes.

García-Peñarrubia et al. [30] have also proposed a theoretical (mathematical) model regarding immune-receptor trafficking processes applying linear differential equations, similar to the study by Dee and Shuler [29]. The study by García-Peñarrubia et al. [30] indicates that the amount of the ligand-receptor complex shows a transient increase followed by a decrease with time similar to the result shown in the present study in a case of the discriminant of Eq. (11) with real roots ($D > 0$ in Eq. (14)). This mathematical model [30] proposes no recycling process similar to the report by Dee and Shuler [29]. Thus, as mentioned above, it is unquestionable that a mathematical model dealing with recycle processes propose should be proposed, then the present study proposes the three-state model enabling us to simulate recycling processes.

Another study by Khailaie et al. [31] has analyzed recycling processes of a receptor, cytotoxic T-lymphocyte-associated protein-4 (CTLA-4) consisting of six states with a mathematical method. They [31] have described changes of amounts of CTLA-4 using differential equations. Similar to the result in a case of the discriminant of Eq. (11) with real roots ($D > 0$ in Eq. (14)) shown in the present study, the time-dependent change of CTLA-4 is expressed by two exponential equations [31]. To solve differential equations, they [31] have used roots of a quadratic equation similar to Eq. (11) in the present study. The simulation represented in the study [31] indicates that the amount of CTLA-4 in each state respectively shows a transient increase or decrease followed by a decrease or increase considering only real numbers but not complex numbers as roots of a quadratic, characteristic Eq. ($A18$) for differential Eqs. ($A14$), ($A15$) or ($A16$) (*i.e.*, in a case of $n = 0$ for a characteristic Eq. ($A17$); see Appendix). On one hand, the experimentally detected value of CTLA-4 amounts on cell surface represented in the study [31] shows oscillatory changes. In the report [31], the oscillatory change would be treated as experimental errors. Thus, the study [31] concludes that the amount of CTLA-4 on cell surface decreases monotonically with the time. Based on the conclusion [31], the experimentally detected value of CTLA-4 amounts on cell surface is fitted using an equation similar to the method reported in the present study with real number roots. Further, the simulation shown in the study [31] has indicated that the amount of CTLA-4 in each state respectively show a transient increase or decrease followed by a decrease or increase using real numbers but not

complex numbers as roots of a quadratic, characteristic Eq. (*A*18) for differential Eqs. (*A*14), (*A*15) or (*A*16) (*i.e.*, in a case of $n = 0$ for a characteristic Eq. (*A*17); see Appendix). The experimentally observed amount of CTLA-4 in each state indeed shows oscillatory changes with the time [31]. Nevertheless, the simulation shows no oscillatory change [31]. This means that complex numbers as roots of a quadratic, characteristic Eq. (*A*18) for differential Eqs. (*A*14), (*A*15) or (*A*16) are essentially required to simulate oscillatory changes in various cellular and molecular activities enabling living bodies, organs and cells to keep stabilized internal environments, so called 'homeostasis'. For example, the oscillatory change in the membrane potential of pancreatic ß cells is essentially required for insulin secretion responding to elevation of blood glucose, keeping blood glucose at a stable level [18,32]. These observations suggest that a mathematical model simulating oscillatory phenomena with the involvement of complex number roots for Eq. (11) is highly useful to recognize various types of biological phenomena, enabling us to obtain detailed understandings on biological activities and their regulation.

In the present study, we propose a three-state mathematical model. Therefore, it is questionable if we could solve other models containing the states more than three; *e.g.*, a four-state mathematical model, and other models containing even much larger number of states than four. The solution for the model containing the states more than three is important to clarify biological phenomena. However, the aim of the present study is to solve the simple three-state mathematical model. Thus, in the present study, we first show the solution of the three-state mathematical model, although it is unquestionable that we should solve mathematical models containing the states more than three in future studies.

Taken together, these studies [29–31] support the conclusion in a case of real number roots for a quadratic, characteristic Eq. (11) (*i.e.*, a case of $D > 0$: $D = (k_I + k_E + k_R)^2 - 4(k_Ik_E + k_Ek_R + k_Rk_I) = 2k_I^2 + k_E^2 + k_R^2 - 2(k_Ik_E + k_Ek_R + k_Rk_I)$ is the discriminant of quadratic, characteristic Eq. (11) or (*A*18) (see Appendix)) shown in the present study (see Appendix). Further studies combing biological experimental observations with mathematical methods proposed in the present study are required to analyze biological phenomena, which frequently show oscillatory changes essentially required for homeostasis in various important bodily and cellular functions.

5. Conclusions

The present study proposes a three-state model in intracellular protein trafficking using differential equations. A quadratic equation, $r^2 + (k_I + k_E + k_R)r + (k_Ik_E + k_Ik_R + +k_Ek_R) = 0$, is essentially important to clarify the time-dependent change in the amount of proteins staying at each state. 'Complex' number solutions of the quadratic equation play essentially important roles in appearance of oscillatory time-dependent changes in the protein trafficking, suggesting that 'complex' number would be essentially required for biological phenomena showing time-dependent oscillatory changes.

Funding

This work was supported by Grants-in-Aid from Japan Society of the Promotion of Science (JSPS KAKENHI 18H03182 and 21H03368 to YM).

CRediT authorship contribution statement

Yoshinori Marunaka: Conceptualization, Writing - original draft, Writing - review & editing, Funding acquisition. **Katsumi Yagi:** Writing - original draft, Writing - review & editing.

Declaration of Competing Interest

The authors declare that they have no known competing financial interests or personal relationships that could have appeared to influence the work reported in this paper.

Appendix

Index of Appendix

Appendix I: Calculating methods solving differential equations without matrix application

Appendix II: Calculating methods solving differential equations using matrix application

Appendix I: Calculating methods solving differential equations without matrix application

Appendix I-1: Solution of differential equations

We describe the process how to obtain Eqs. (5), (6), (7), (8), (9), (10) and (11) below.

$$\frac{dIns(t)}{dt} = -k_IIns(t) + k_RRec(t) \tag{A1}$$

$$\frac{dPlas(t)}{dt} = -k_EPlas(t) + k_IIns(t) \tag{A2}$$

$$\frac{dRec(t)}{dt} = -k_RRec(t) + k_EPlas(t) \tag{A3}$$

where t is the time after application of stimulation affecting any trafficking rate, k_I,k_E or k_R: $Ins(t) \geqq 0$, $Plas(t) \geqq 0$, $Rec(t) \geqq 0$, and $k_I > 0$, $k_E > 0$ and $k_R > 0$.

Eq. (*A*4) is obtained from Eq. (*A*1).

$$\frac{dIns(t)}{dt} + k_IIns(t) - k_RRec(t) = 0 \tag{A4}$$

Eq. (*A*5) is obtained by differentiating Eq. (*A*4).

$$\frac{d^2Ins(t)}{dt^2} + k_I\frac{dIns(t)}{dt} - k_R\frac{dRec(t)}{dt} = 0 \tag{A5}$$

Eq. (*A*6) is obtained by substituting Eq. (*A*3) into Eq. (*A*5).

$$\frac{d^2Ins(t)}{dt^2} + k_I\frac{dIns(t)}{dt} + k_R(k_RRec(t) - k_EPlas(t)) = 0 \tag{A6}$$

Eq. (*A*7) is obtained by substituting $k_RRec(t)$ with Eq. (*A*1) into Eq. (*A*6).

$$\frac{d^2Ins(t)}{dt^2} + (k_R + k_I)\frac{dIns(t)}{dt} + k_R(k_IIns(t) - k_EPlas(t)) = 0 \tag{A7}$$

Eq. (*A*8) is obtained by substituting Eq. (*A*2) ($k_IIns(t) - k_EPlas(t)$) into Eq. (*A*7).

$$\frac{d^2Ins(t)}{dt^2} + (k_R+k_I)\frac{dIns(t)}{dt} + k_R\frac{dPlas(t)}{dt} = 0 \tag{A8}$$

Eq. (*A*9) is obtained from Eq. (*A*8).

$$-k_R\frac{dPlas(t)}{dt} = \frac{d^2Ins(t)}{dt^2} + (k_R + k_I)\frac{dIns(t)}{dt} \tag{A9}$$

Eq. (*A*10) is obtained by differentiating Eq. (*A*9).

$$\frac{d^3Ins(t)}{dt^3} + (k_R + k_I)\frac{d^2Ins(t)}{dt^2} + k_Rk_I\frac{dIns(t)}{dt} - k_Ek_R\frac{dPlas(t)}{dt} = 0 \tag{A10}$$

Eq. (*A*11) is obtained by substituting Eq. (*A*9) into the differentiated Eq. (*A*10).

$$\frac{d^3Ins(t)}{dt^3} + (k_R + k_I)\frac{d^2Ins(t)}{dt^2} + k_R k_I \frac{dIns(t)}{dt} + k_E\left(\frac{d^2Ins(t)}{dt^2} + (k_R + k_I)\frac{dIns(t)}{dt}\right) = 0 \quad (A11)$$

Thus, Eq. (A12) regarding $Ins(t)$ is obtained from Eq. (A11), and similarly Eqs. (A13) and (A14) regarding $Plas(t)$ and $Rec(t)$ are respectively obtained as follows.

$$\frac{d^3Ins(t)}{dt^3} + (k_I + k_R + k_E)\frac{d^2Ins(t)}{dt^2} + (k_I k_E + k_E k_R + k_R k_I)\frac{dIns(t)}{dt} = 0 \quad (A12)$$

$$\frac{d^3Plas(t)}{dt^3} + (k_I + k_R + k_E)\frac{d^2Plas(t)}{dt^2} + (k_I k_E + k_E k_R + k_R k_I)\frac{dPlas(t)}{dt} = 0 \quad (A13)$$

$$\frac{d^3Rec(t)}{dt^3} + (k_I + k_R + k_E)\frac{d^2Rec(t)}{dt^2} + (k_I k_E + k_E k_R + k_R k_I)\frac{dRec(t)}{dt} = 0 \quad (A14)$$

The characteristic equation for cubic differential Eqs. (A12), (A13) and (A14) is Eq. (A15).

$$\lambda^3 + (k_I + k_R + k_E)\lambda^2 + (k_I k_E + k_E k_R + k_R k_I)\lambda = (\lambda - l)(\lambda - m)(\lambda - n) = 0 \quad (A15)$$

where l, m and n ($n = 0$) are roots of Eq. (A15). Thus, l and m are roots of quadratic Eq. (A16).

$$\lambda^2 + (k_I + k_R + k_E)\lambda + (k_I k_E + k_E k_R + k_R k_I) = (\lambda - l)(\lambda - m) = 0 \quad (A16)$$

Thus, $Ins(t)$, $Plas(t)$ and $Rec(t)$ (see Eqs. (A1), (A2) and (A3)) can be respectively described as Eqs. (A17), (A18) and (A19).

$$Ins(t) = C_{1I}e^{lt} + C_{2I}e^{mt} + C_{3I}e^{nt} \quad (A17)$$

$$Plas(t) = C_{1P}e^{lt} + C_{2P}e^{mt} + C_{3P}e^{nt} \quad (A18)$$

$$Rec(t) = C_{1R}e^{lt} + C_{2R}e^{mt} + C_{3R}e^{nt} \quad (A19)$$

where C_{1I}, C_{2I}, C_{3I}, C_{1P}, C_{2P}, C_{3P}, C_{1R}, C_{2R} and C_{3R} are constant, and l, m and n are roots of Eq. (A15). We substitute Eqs. (A17) and (A19) into Eq. (1), obtaining Eq. (A20).

$$\frac{dIns(t)}{dt} = lC_{1I}e^{lt} + mC_{2I}e^{mt} + nC_{3I}e^{nt} = -k_I Ins(t) + k_R Rec(t) = -k_I\left(C_{1I}e^{lt} + C_{2I}e^{mt} + C_{3I}e^{nt}\right) + k_R\left(C_{1R}e^{lt} + C_{2R}e^{mt} + C_{3R}e^{nt}\right) \quad (A20)$$

Eq. (A21) is obtained from Eq. (A20).

$$(k_I + l)C_{1I}e^{lt} + (k_I + m)C_{2I}e^{mt} + (k_I + n)C_{3I}e^{nt} = k_R C_{1R}e^{lt} + k_R C_{2R}e^{mt} + k_R C_{3R}e^{nt} \quad (A21)$$

Thus, Eqs. (A22), (A23) and (A24) are obtained from Eq. (A21).

$$C_{1R} = \frac{k_I + l}{k_R}C_{1I} \quad (A22)$$

$$C_{2R} = \frac{k_I + m}{k_R}C_{2I} \quad (A23)$$

$$C_{3R} = \frac{k_I + n}{k_R}C_{3I} \quad (A24)$$

Similarly, Eq. (A25) and (A26) is obtained from Eqs. (A2), (A18) and (A21).

$$\frac{dPlas(t)}{dt} = lC_{1P}e^{lt} + mC_{2P}e^{mt} + nC_{3P}e^{nt} = -k_E\left(C_{1P}e^{lt} + C_{2P}e^{mt} + C_{3P}e^{nt}\right) + k_I\left(C_{1I}e^{lt} + C_{2I}e^{mt} + C_{3I}e^{nt}\right) \quad (A25)$$

Eq. (A26) is obtained from Eq. (A25).

$$(k_E + l)C_{1P}e^{lt} + (k_E + m)C_{2P}e^{mt} + (k_E + n)C_{3P}e^{nt} = k_I\left(C_{1I}e^{lt} + C_{2I}e^{mt} + C_{3I}e^{nt}\right) \quad (A26)$$

Thus, Eqs. (A27), (A28) and (A29) are obtained from Eq. (A26).

$$C_{1I} = \frac{k_E + l}{k_I}C_{1P} \quad (A27)$$

$$C_{2I} = \frac{k_E + m}{k_I}C_{2P} \quad (A28)$$

$$C_{3I} = \frac{k_E + n}{k_I}C_{3P} \quad (A29)$$

Eq. (A30) is obtained from Eqs. (A22) and (A27). Similarly, Eq. (A31) is obtained from Eqs. (A23) and (A28). Further, Eq. (A32) is obtained from Eqs. (A24) and (A29).

$$C_{1R} = \frac{(k_I + l)(k_E + l)}{k_R k_I}C_{1P} \quad (A30)$$

$$C_{2R} = \frac{(k_I + m)(k_E + m)}{k_R k_I}C_{2P} \quad (A31)$$

$$C_{3R} = \frac{(k_I + n)(k_E + n)}{k_R k_I}C_{3P} \quad (A32)$$

We define as follows.

$$C_1 = C_{1P} \quad (A33)$$

$$C_2 = C_{2P} \quad (A34)$$

$$C_3 = C_{3P} \quad (A35)$$

Eq. (A17) is described as Eq. (A36) using (A27), (A28), (A29), (A33), (A34) and (A35).

$$Ins(t) = C_1\frac{(k_E + l)}{k_I}e^{lt} + C_2\frac{(k_E + m)}{k_I}e^{mt} + C_3\frac{(k_E + n)}{k_I}e^{nt} \quad (A36)$$

Eq. (A18) is described as Eq. (A37) using (A33), (A34) and (A35).

$$Plas(t) = C_1e^{lt} + C_2e^{mt} + C_3e^{nt} \quad (A37)$$

Eq. (A19) is described as Eq. (A38) using (A30), (A31), (A32), (A33), (A34) and (A35).

$$Rec(t) = C_1\frac{(k_I + l)(k_E + l)}{k_R k_I}e^{lt} + C_2\frac{(k_I + m)(k_E + m)}{k_R k_I}e^{mt} + C_3\frac{(k_I + n)(k_E + n)}{k_R k_I}e^{nt} \quad (A38)$$

Here, C_1, C_2 and C_3 are determined as followed.

When $t = 0$, Eqs. (A36), (A37) and (A38) are respectively described as Eqs. (A39), (A40) and (A41).

$$Ins(0) = C_1\frac{(k_E + l)}{k_I} + C_2\frac{(k_E + m)}{k_I} + C_3\frac{(k_E + n)}{k_I} \quad (A39)$$

$$Plas(0) = C_1 + C_2 + C_3 \quad (A40)$$

$$Rec(0) = C_1\frac{(k_I+l)(k_E+l)}{k_Rk_I} + C_2\frac{(k_I+m)(k_E+m)}{k_Rk_I} + C_3\frac{(k_I+n)(k_E+n)}{k_Rk_I} \quad (A41)$$

Eq. (A42) is obtained from Eq. (A39).

$$k_IIns(0) = C_1(k_E+l) + C_2(k_E+m) + C_3(k_E+n) \quad (A42)$$

Eq. (A43) is obtained from Eq. (A40).

$$(k_E+n)Plas(0) = C_1(k_E+n) + C_2(k_E+n) + C_3(k_E+n) \quad (A43)$$

Eq. (A44) = Eq. (A42) – Eq. (A43)

$$k_IIns(0) - (k_E+n)Plas(0) = C_1((k_E+l)-(k_E+n)) + C_2((k_E+m)-(k_E+n)) = -C_1(n-l) + C_2(m-n) \quad (A44)$$

Eq. (A45) is obtained from Eq. (A42).

$$k_I(k_I+n)Ins(0) = C_1(k_I+n)(k_E+l) + C_2(k_I+n)(k_E+m) + C_3(k_I+n)(k_E+n) \quad (A45)$$

Eq. (A46) is obtained from Eq. (A41).

$$k_Rk_IRec(0) = C_1(k_I+l)(k_E+l) + C_2(k_I+m)(k_E+m) + C_3(k_I+n)(k_E+n) \quad (A46)$$

Eq. (A47) = Eq. (A45) – Eq. (A46)

$$k_I(k_I+n)Ins(0) - k_Rk_IRec(0) = C_1(k_E+l)(n-l) - C_2(k_E+m)(m-n) \quad (A47)$$

Eq. (A48) is obtained from Eq. (A44).

$$(k_E+m)(k_IIns(0) - (k_E+n)Plas(0)) = -C_1(k_E+m)(n-l) + C_2(k_E+m)(m-n) \quad (A48)$$

Eq. (A49) = Eq. (A47) + Eq. (A48)

$$k_I(k_I+k_E+m+n)Ins(0) - (k_E+m)(k_E+n)Plas(0) - k_Rk_IRec(0) = C_1(n-l)(l-m) \quad (A49)$$

Eq. (A50) is obtained from Eq. (A49).

$$C_1 = \frac{1}{(n-l)(l-m)}(k_I(k_I+k_E+m+n)Ins(0) - (k_E+m)(k_E+n)Plas(0) - k_Rk_IRec(0)) \quad (A50)$$

Eq. (A51) is obtained from Eq. (A44).

$$(k_E+l)(k_IIns(0) - (k_E+n)Plas(0)) = -C_1(k_E+l)(n-l) + C_2(k_E+l)(m-n) \quad (A51)$$

Eq. (A52) = Eq. (A51) + Eq. (A47)

$$(k_E+l)(k_IIns(0) - (k_E+n)Plas(0)) + k_I(k_I+n)Ins(0) - k_Rk_IRec(0) = C_2(l-m)(m-n) \quad (A52)$$

Eq. (A53) is obtained from (A52).

$$C_2 = \frac{1}{(l-m)(m-n)}(k_I(k_I+k_E+n+l)Ins(0) - (k_E+l)(k_E+n)Plas(0) - k_Rk_IRec(0)) \quad (A53)$$

Eq. (A54) is obtained from Eq. (A40).

$$(k_E+m)Plas(0) = C_1(k_E+m) + C_2(k_E+m) + C_3(k_E+m) \quad (A54)$$

Eq. (A55) = Eq. (A42) – Eq. (A54).

$$k_IIns(0) - (k_E+m)Plas(0) = C_1(l-m) - C_3(m-n) \quad (A55)$$

Eq. (A56) is obtained from Eq. (A55) (Eq. (A56) = Eq. (A55) × (k_E+l)).

$$k_I(k_E+l)Ins(0) - (k_E+l)(k_E+m)Plas(0) = C_1(k_E+l)(l-m) - C_3(k_E+l)(m-n) \quad (A56)$$

Eq. (A57) = Eq. (A52) - Eq. (A46)

$$k_I(k_I+m)Ins(0) - k_Rk_IRec(0) = C_1(k_E+l)((k_I+m) - (k_I+l)) + C_3(k_E+n)(k_I+m) - (k_I+n)) = -C_1(k_E+l)(l-m) + C_3(k_E+n)(m-n) \quad (A57)$$

Eq. (A58) = Eq. (A56) + Eq. (A57)

$$k_I(k_I+m)Ins(0) - k_Rk_IRec(0) + k_I(k_E+l)Ins(0) - (k_E+l)(k_E+m)Plas(0) = C_3(m-n)(n-l) \quad (A58)$$

Eq. (A59) is obtained from Eq. (A58).

$$C_3 = \frac{1}{(m-n)(n-l)}(k_I(k_I+k_E+l+m)Ins(0) - (k_E+l)(k_E+m)Plas(0) - k_Rk_IRec(0)) \quad (A59)$$

Thus, C_1, C_2 and C_3 are respectively described in Eqs. (A60), (A61) and (A62) (see Eqs. (8), (9) and (10)).

$$C_1 = \frac{k_I(k_I+k_E+m+n)Ins(0) - (k_E+m)(k_E+n)Plas(0) - k_Rk_IRec(0)}{(n-l)(l-m)} \quad (A60)$$

$$C_2 = \frac{k_I(k_I+k_E+n+l)Ins(0) - (k_E+n)(k_E+l)Plas(0) - k_Rk_IRec(0)}{(l-m)(m-n)} \quad (A61)$$

$$C_3 = \frac{k_I(k_I+k_E+l+m)Ins(0) - (k_E+l)(k_E+m)Plas(0) - k_Rk_IRec(0)}{(m-n)(n-l)} \quad (A62)$$

Appendix I-2: Determination of $\boldsymbol{C}_1$, $\boldsymbol{C}_2$ and $\boldsymbol{C}_3$

Appendix I-2-a: In a case of the discriminant Eq. (14) for Eq. (11), $\boldsymbol{D} > 0$:

When $n = 0$ in Eqs. (A60), (A61) and (A62), Eqs. (A60), (A61) and (A62) are respectively described as Eqs. (A63), (A64) and (A65).

$$C_1 = \frac{k_I(k_I+k_E+m)Ins(0) - (k_E+m)k_EPlas(0) - k_Rk_IRec(0)}{-l(l-m)} \quad (A63)$$

$$C_2 = \frac{k_I(k_I+k_E+l)Ins(0) - k_E(k_E+l)Plas(0) - k_Rk_IRec(0)}{m(l-m)} \quad (A64)$$

$$C_3 = \frac{k_I(k_I+k_E+l+m)Ins(0) - (k_E+l)(k_E+m)Plas(0) - k_Rk_IRec(0)}{-lm} \quad (A65)$$

where l and m are roots for Eq. (A16) and real numbers. Since l and m are roots for Eq. (A16) and real numbers, l and m are respectively described using a and b as follows (a and b are real numbers).

$$l = a - b = \frac{-(k_I+k_E+k_R) - \sqrt{(k_I+k_E+k_R)^2 - 4(k_Ik_E+k_Ek_R+k_Rk_I)}}{2} \quad (A66)$$

$$m = a + b = \frac{-(k_I+k_E+k_R) + \sqrt{(k_I+k_E+k_R)^2 - 4(k_Ik_E+k_Ek_R+k_Rk_I)}}{2} \quad (A67)$$

$$a = -\frac{k_I+k_E+k_R}{2} \quad (A68)$$

$$b = \frac{\sqrt{(k_I + k_E + k_R)^2 - 4(k_I k_E + k_E k_R + k_R k_I)}}{2} \quad \text{(A69)}$$

Eq. (*A*63) is described as follows using Eqs. (*A*66), (*A*67), (*A*68) and (*A*69).

$$C_1 = -\frac{(k_I + k_E + k_R) - \sqrt{(k_I + k_E + k_R)^2 - 4(k_I k_E + k_E k_R + k_R k_I)}}{4(k_I k_E + k_E k_R + k_R k_I)\sqrt{(k_I + k_E + k_R)^2 - 4(k_I k_E + k_E k_R + k_R k_I)}} \times \left[k_I\left\{(k_I + k_E - k_R) + \sqrt{(k_I + k_E + k_R)^2 - 4(k_I k_E + k_E k_R + k_R k_I)}\right\}Ins(0) + k_E\left\{(k_I - k_E + k_R) - \sqrt{(k_I + k_E + k_R)^2 - 4(k_I k_E + k_E k_R + k_R k_I)}\right\}Plas(0) - 2k_R k_I Rec(0)\right] \quad \text{(A70)}$$

Eq. (*A*64) is described as follows using Eqs. (*A*66), (*A*67), (*A*68) and (*A*69).

$$C_2 = \frac{(k_I + k_E + k_R) + \sqrt{(k_I + k_E + k_R)^2 - 4(k_I k_E + k_E k_R + k_R k_I)}}{4(k_I k_E + k_E k_R + k_R k_I)\sqrt{(k_I + k_E + k_R)^2 - 4(k_I k_E + k_E k_R + k_R k_I)}} \times \left[k_I\left\{(k_I + k_E - k_R) - \sqrt{(k_I + k_E + k_R)^2 - 4(k_I k_E + k_E k_R + k_R k_I)}\right\}Ins(0) + k_E\left\{(k_I - k_E + k_R) + \sqrt{(k_I + k_E + k_R)^2 - 4(k_I k_E + k_E k_R + k_R k_I)}\right\}Plas(0) - 2k_R k_I Rec(0)\right] \quad \text{(A71)}$$

Eq. (*A*65) is described as follows using Eqs. (*A*66), (*A*67), (*A*68) and (*A*69).

$$C_3 = \frac{k_R k_I}{k_I k_E + k_E k_R + k_R k_I}(Ins(0) + Plas(0) + Rec(0)) \quad \text{(A72)}$$

Further, C_{1I}, C_{2I} and C_{3I} are described as follows using Eqs. (*A*27), (*A*28), (*A*29), (*A*33), (*A*34), (*A*35), (70), (71) and (72).

$$C_{1I} = \frac{(k_I + k_E + k_R) - \sqrt{(k_I + k_E + k_R)^2 - 4(k_I k_E + k_E k_R + k_R k_I)}}{8k_I(k_I k_E + k_E k_R + k_R k_I)\sqrt{(k_I + k_E + k_R)^2 - 4(k_I k_E + k_E k_R + k_R k_I)}} \times \left[k_I\left\{(k_I + k_E - k_R) + \sqrt{(k_I + k_E + k_R)^2 - 4(k_I k_E + k_E k_R + k_R k_I)}\right\}Ins(0) + k_E\left\{(k_I - k_E + k_R) - \sqrt{(k_I + k_E + k_R)^2 - 4(k_I k_E + k_E k_R + k_R k_I)}\right\}Plas(0) - 2k_R k_I Rec(0)\right]\left((k_I - k_E + k_R) + \sqrt{(k_I + k_E + k_R)^2 - 4(k_I k_E + k_E k_R + k_R k_I)}\right) \quad \text{(A73)}$$

$$C_{2I} = -\frac{(k_I + k_E + k_R) + \sqrt{(k_I + k_E + k_R)^2 - 4(k_I k_E + k_E k_R + k_R k_I)}}{8k_I(k_I k_E + k_E k_R + k_R k_I)\sqrt{(k_I + k_E + k_R)^2 - 4(k_I k_E + k_E k_R + k_R k_I)}} \times \left[k_I\left\{(k_I + k_E - k_R) - \sqrt{(k_I + k_E + k_R)^2 - 4(k_I k_E + k_E k_R + k_R k_I)}\right\}Ins(0) + k_E\left\{(k_I - k_E + k_R) + \sqrt{(k_I + k_E + k_R)^2 - 4(k_I k_E + k_E k_R + k_R k_I)}\right\}Plas(0) - 2k_R k_I Rec(0)\right]\left((k_I - k_E + k_R) - \sqrt{(k_I + k_E + k_R)^2 - 4(k_I k_E + k_E k_R + k_R k_I)}\right) \quad \text{(A74)}$$

$$C_{3I} = \frac{k_E k_R}{k_I k_E + k_E k_R + k_R k_I}(Ins(0) + Plas(0) + Rec(0)) \quad \text{(A75)}$$

C_{1P}, C_{2P} and C_{3P} are also described as follows using Eqs. (*A*33), (*A*34), (*A*70), (*A*71) and (*A*72).

$$C_{1P} = -\frac{(k_I + k_E + k_R) - \sqrt{(k_I + k_E + k_R)^2 - 4(k_I k_E + k_E k_R + k_R k_I)}}{4(k_I k_E + k_E k_R + k_R k_I)\sqrt{(k_I + k_E + k_R)^2 - 4(k_I k_E + k_E k_R + k_R k_I)}} \times \left[k_I\left\{(k_I + k_E - k_R) + \sqrt{(k_I + k_E + k_R)^2 - 4(k_I k_E + k_E k_R + k_R k_I)}\right\}Ins(0) + k_E\left\{(k_I - k_E + k_R) - \sqrt{(k_I + k_E + k_R)^2 - 4(k_I k_E + k_E k_R + k_R k_I)}\right\}Plas(0) - 2k_R k_I Rec(0)\right] \quad \text{(A76)}$$

$$C_{2P} = \frac{(k_I + k_E + k_R) + \sqrt{(k_I + k_E + k_R)^2 - 4(k_I k_E + k_E k_R + k_R k_I)}}{4(k_I k_E + k_E k_R + k_R k_I)\sqrt{(k_I + k_E + k_R)^2 - 4(k_I k_E + k_E k_R + k_R k_I)}} \times \left[k_I\left\{(k_I + k_E - k_R) - \sqrt{(k_I + k_E + k_R)^2 - 4(k_I k_E + k_E k_R + k_R k_I)}\right\}Ins(0) + k_E\left\{(k_I - k_E + k_R) + \sqrt{(k_I + k_E + k_R)^2 - 4(k_I k_E + k_E k_R + k_R k_I)}\right\}Plas(0) - 2k_R k_I Rec(0)\right] \quad \text{(A77)}$$

$$C_{3P} = C_3 = \frac{k_R k_I}{k_I k_E + k_E k_R + k_R k_I}(Ins(0) + Plas(0) + Rec(0)) \quad \text{(A78)}$$

Further, C_{1R}, C_{2R} and C_{3R} are described as follows using Eqs. (*A*30), (*A*31), (*A*32), (*A*76), (*A*77) and (*A*78).

$$C_{1R} = \frac{(k_I + k_E + k_R) - \sqrt{(k_I + k_E + k_R)^2 - 4(k_I k_E + k_E k_R + k_R k_I)}}{16k_R k_I(k_I k_E + k_E k_R + k_R k_I)\sqrt{(k_I + k_E + k_R)^2 - 4(k_I k_E + k_E k_R + k_R k_I)}} \times \left[k_I\left\{(k_I + k_E - k_R) + \sqrt{(k_I + k_E + k_R)^2 - 4(k_I k_E + k_E k_R + k_R k_I)}\right\}Ins(0) + k_E\left\{(k_I - k_E + k_R) - \sqrt{(k_I + k_E + k_R)^2 - 4(k_I k_E + k_E k_R + k_R k_I)}\right\}Plas(0) - 2k_R k_I Rec(0)\right]\left((k_I - k_E - k_R) - \sqrt{(k_I + k_E + k_R)^2 - 4(k_I k_E + k_E k_R + k_R k_I)}\right) \times \left((k_I - k_E + k_R) + \sqrt{(k_I + k_E + k_R)^2 - 4(k_I k_E + k_E k_R + k_R k_I)}\right) \quad \text{(A79)}$$

$$C_{2R} = -\frac{(k_I + k_E + k_R) + \sqrt{(k_I + k_E + k_R)^2 - 4(k_I k_E + k_E k_R + k_R k_I)}}{16k_R k_I(k_I k_E + k_E k_R + k_R k_I)\sqrt{(k_I + k_E + k_R)^2 - 4(k_I k_E + k_E k_R + k_R k_I)}} \times \left[k_I\left\{(k_I + k_E - k_R) - \sqrt{(k_I + k_E + k_R)^2 - 4(k_I k_E + k_E k_R + k_R k_I)}\right\}Ins(0) + k_E\left\{(k_I - k_E + k_R) + \sqrt{(k_I + k_E + k_R)^2 - 4(k_I k_E + k_E k_R + k_R k_I)}\right\}Plas(0) - 2k_R k_I Rec(0)\right]\left((k_I - k_E - k_R) + \sqrt{(k_I + k_E + k_R)^2 - 4(k_I k_E + k_E k_R + k_R k_I)}\right) \times \left((k_I - k_E + k_R) - \sqrt{(k_I + k_E + k_R)^2 - 4(k_I k_E + k_E k_R + k_R k_I)}\right) \quad \text{(A80)}$$

$$C_{3R} = \frac{k_E}{2(k_I k_E + k_E k_R + k_R k_I)} \times \left((k_I - k_E - k_R) + \sqrt{(k_I + k_E + k_R)^2 - 4(k_I k_E + k_E k_R + k_R k_I)}\right)(Ins(0) + Plas(0) + Rec(0)) \quad \text{(A81)}$$

Appendix I-2-b: In a case of the discriminant Eq. (14) for Eq. (11), $\boldsymbol{D} < 0$:

When $n = 0$ in Eqs. (*A*60), (*A*61) and (*A*62), Eqs. (*A*60), (*A*61) and (*A*62) are described as Eqs. (*A*82), (*A*83) and (*A*84).

$$C_1 = \frac{k_I(k_I + k_E + m)Ins(0) - (k_E + m)k_E Plas(0) - k_R k_I Rec(0)}{-l(l - m)} \quad \text{(A82)}$$

$$C_2 = \frac{k_I(k_I + k_E + l)Ins(0) - k_E(k_E + l)Plas(0) - k_R k_I Rec(0)}{m(l - m)} \quad \text{(A83)}$$

$$C_3 = \frac{k_I(k_I + k_E + l + m)Ins(0) - (k_E + l)(k_E + m)Plas(0) - k_R k_I Rec(0)}{-lm} \tag{A84}$$

Where l and m are roots for Eq. (A16) and l and m are complex numbers. Thus, l and m are respectively described using a and b as follows (a and b are real numbers).

$$l = a - ib = \frac{-(k_I + k_E + k_R) - i\sqrt{4(k_I k_E + k_E k_R + k_R k_I) - (k_I + k_E + k_R)^2}}{2} \tag{A85}$$

$$m = a + ib = \frac{-(k_I + k_E + k_R) + i\sqrt{4(k_I k_E + k_E k_R + k_R k_I) - (k_I + k_E + k_R)^2}}{2} \tag{A86}$$

$$a = -\frac{k_I + k_E + k_R}{2} \tag{A87}$$

$$b = \frac{\sqrt{4(k_I k_E + k_E k_R + k_R k_I) - (k_I + k_E + k_R)^2}}{2} \tag{A88}$$

Here, next step is to confirm if C_1 and C_2 would be conjugate. Eq. (A82) is described as follows using Eqs. (A85), (A86), (A87) and (A88).

$$\begin{aligned} C_1 = {} & \frac{-k_R k_I Ins(0) + k_E(k_I + k_R)Plas(0) - k_R k_I Rec(0)}{2(k_I k_E + k_E k_R + k_R k_I)} \\ & - \frac{i}{2(k_I k_E + k_E k_R + k_R k_I)\sqrt{4(k_I k_E + k_E k_R + k_R k_I) - (k_I + k_E + k_R)^2}} \\ & \times \Big[k_I\Big({k_R}^2 - 2k_I k_E - k_E k_R - k_R k_I\Big)Ins(0) \\ & -k_E\Big({k_I}^2 + {k_R}^2 - k_I k_E - k_E k_R\Big)Plas(0) + k_R k_I(k_I + k_E + k_R)Rec(0)\Big] \end{aligned} \tag{A89}$$

Eq. (A83) is described as follows using Eqs. (A85), (A86), (A87) and (A88).

$$\begin{aligned} C_2 = {} & \frac{-k_I k_R Ins(0) + k_E(k_I + k_R)Plas(0) - k_R k_I Rec(0)}{2(k_I k_E + k_E k_R + k_R k_I)} \\ & + \frac{i}{2(k_I k_E + k_E k_R + k_R k_I)\sqrt{4(k_I k_E + k_E k_R + k_R k_I) - (k_I + k_E + k_R)^2}} \\ & \times \Big[k_I\Big({k_R}^2 - 2k_I k_E - k_E k_R - k_R k_I\Big)Ins(0) \\ & -k_E\Big({k_I}^2 + {k_R}^2 - k_I k_E - k_E k_R\Big)Plas(0) + k_R k_I(k_I + k_E + k_R)Rec(0)\Big] \end{aligned} \tag{A90}$$

Thus, C_1 and C_2 are conjugate (see Eqs. (A89) and (A90)). When we describe C_1 and C_2 as Eqs. (A91) and (A92) respectively, g and h are respectively expressed in Eqs. (A93) and (A94) (g and h are real numbers).

$$C_1 = g + ih \tag{A91}$$

$$C_2 = g - ih \tag{A92}$$

$$g = \frac{-k_I k_R Ins(0) + k_E(k_I + k_R)Plas(0) - k_R k_I Rec(0)}{2(k_I k_E + k_E k_R + k_R k_I)} \tag{A93}$$

$$\begin{aligned} h = {} & -\frac{1}{2(k_I k_E + k_E k_R + k_R k_I)\sqrt{4(k_I k_E + k_E k_R + k_R k_I) - (k_I + k_E + k_R)^2}} \\ & \times \Big(k_I\Big({k_R}^2 - 2k_I k_E - k_E k_R - k_R k_I\Big)Ins(0) \\ & -k_E\Big({k_I}^2 + {k_R}^2 - k_I k_E - k_E k_R\Big)Plas(0) + k_R k_I(k_I + k_E + k_R)Rec(0)\Big) \end{aligned} \tag{A94}$$

Based on Eqs. (A17), (A27), (A28), (A33), (A34), (A89), (A90), (A91) and (A92), we obtain Eqs. (A95) and (A96).

$$C_{1I} = \frac{k_E + l}{k_I}(g + ih) = g_I + ih_I \tag{A95}$$

$$C_{2I} = \frac{k_E + m}{k_I}(g - ih) = g_I - ih_I \tag{A96}$$

Then, Eqs. (A97) and (A98) are obtained (c.f., Eqs. (A85) and (A86).

$$C_{1I} = \frac{1}{k_I}[(gk_E + ag + bh) + i(hk_E + ah - bg)] \tag{A97}$$

$$C_{2I} = \frac{1}{k_I}[(gk_E + ag + bh) - i(hk_E + ah - bg)] \tag{A98}$$

Thus, C_{1I} and C_{2I} are conjugate. Then, g_I and h_I are respectively expressed as Eqs. (A99) and (A100).

$$g_I = \frac{gk_E + ag + bh}{k_I} \tag{A99}$$

$$h_I = \frac{hk_E + ah - bg}{k_I} \tag{A100}$$

Based on Eqs. (A18), (A33), (A34), (A89), (A90) (A91) and (A92), we obtain Eqs. (A101) and (A102).

$$C_{1P} = C_1 = g + ih \tag{A101}$$

$$C_{2P} = C_2 = g - ih \tag{A102}$$

Thus, C_{1P} and C_{2P} are conjugate.

Based on Eqs. (A19), (A30), (A31), (A33), (A34), (A89), (A90), (A91) and (A92), we obtain Eqs. (A103) and (A104).

$$C_{1R} = \frac{(k_I + l)(k_E + l)}{k_R k_I}(g + ih) = g_R + ih_R \tag{A103}$$

$$C_{2R} = \frac{(k_I + m)(k_E + m)}{k_R k_I}(g_R - ih_R) = g_R - ih_R \tag{A104}$$

Then, Eqs. (A105) and (A106) are obtained.

$$\begin{aligned} C_{1R} = {} & \frac{1}{k_R k_I}[\{(k_I + a)(gk_E + ag + bh) + b(hk_E + ah - bg)\} \\ & + i\{(k_I + a)(hk_E + ah - bg) - b(gk_E + ag + bh)\}] \end{aligned} \tag{A105}$$

$$\begin{aligned} C_{1R} = {} & \frac{1}{k_R k_I}[\{(k_I + a)(gk_E + ag + bh) + b(hk_E + ah - bg)\} \\ & - i\{(k_I + a)(hk_E + ah - bg) - b(gk_E + ag + bh)\}] \end{aligned} \tag{A106}$$

Thus, C_{1R} and C_{1R} are conjugate. Then, Eqs. (A107) and (A108) are obtained.

$$g_R = \frac{(k_I + a)(gk_E + ag + bh) + b(hk_E + ah - bg)}{k_R k_I} \tag{A107}$$

$$h_R = \frac{(k_I + a)(hk_E + ah - bg) - b(gk_E + ag + bh)}{k_R k_I} \tag{A108}$$

Based on Eqs. (A84), (A85), (A86), (A87), and (A88), we obtain Eq. (A109).

$$C_3 = \frac{k_R k_I}{k_I k_E + k_E k_R + k_R k_I}(Ins(0) + Plas(0) + Rec(0)) \tag{A109}$$

Thus, based on Eqs. (A29), (A32), (A35) and (A109), we obtain Eqs. (A110) and (A111) with $n = 0$.

$$C_{3I} = \frac{k_E k_R}{k_I k_E + k_E k_R + k_R k_I}(Ins(0) + Plas(0) + Rec(0)) \quad \text{(A110)}$$

$$C_{3P} = \frac{k_R k_I}{k_I k_E + k_E k_R + k_R k_I}(Ins(0) + Plas(0) + Rec(0)) \quad \text{(A111)}$$

$$C_{3R} = \frac{k_I k_E}{k_I k_E + k_E k_R + k_R k_I}(Ins(0) + Plas(0) + Rec(0)) \quad \text{(A112)}$$

We further describe Eq. (25) in detail as follows.

$$Ins(t) = 2\sqrt{{g_I}^2 + {h_I}^2}\sin(bt + \sigma_I)e^{at} + C_{3I} \quad \text{(A113)}$$

$$Plas(t) = 2\sqrt{{g_P}^2 + {h_P}^2}\sin(bt + \sigma_P)e^{at} + C_{3P} \quad \text{(A114)}$$

$$Rec(t) = 2\sqrt{{g_R}^2 + {h_R}^2}\sin(bt + \sigma_R)e^{at} + C_{3R} \quad \text{(A115)}$$

where σ_I, σ_P and σ_R are defined as follows (see Eqs. (*A*87) and (*A*88) regarding a and b; see Eqs. (A109), (A110) and (A111) regarding C_{3I}, C_{3P} and C_{3R}).

$$\cos\sigma_I = \frac{h_I}{\sqrt{{g_I}^2 + {h_I}^2}} \quad \text{(A116)}$$

$$\sin\sigma_I = \frac{g_I}{\sqrt{{g_I}^2 + {h_I}^2}} \quad \text{(A117)}$$

$$\cos\sigma_P = \frac{h_P}{\sqrt{{g_P}^2 + {h_P}^2}} \quad \text{(A118)}$$

$$\sin\sigma_P = \frac{g_P}{\sqrt{{g_P}^2 + {h_P}^2}} \quad \text{(A119)}$$

$$\cos\sigma_R = \frac{h_R}{\sqrt{{g_R}^2 + {h_R}^2}} \quad \text{(A120)}$$

$$\sin\sigma_R = \frac{g_R}{\sqrt{{g_R}^2 + {h_R}^2}} \quad \text{(A121)}$$

Appendix II: Solving differential equations with matrix application

Appendix II-1: Differential equations

We define the parameters appearing in Fig. 1 as letters in Eq. (*AM*1).

$$\left.\begin{array}{l} x = Ins(t) \\ y = Plas(t) \\ z = Rec(t) \\ a = k_I \\ b = k_E \\ c = k_R \end{array}\right\} \quad \text{(AM1)}$$

$$x' = \frac{dx}{dt} = -ax + cz \quad \text{(AM2)}$$

$$y' = \frac{dy}{dt} = ax - by \quad \text{(AM3)}$$

$$z' = \frac{dz}{dt} = by - cz \quad \text{(AM4)}$$

Here, the constants, a, b and c, are positive, since the model shown in Fig. 1 indicates k_I, k_E and k_R are positive.

The vector x and the matrix M are given as follows:

$$\boldsymbol{x} = \begin{pmatrix} x \\ y \\ z \end{pmatrix} \quad \text{(AM5)}$$

$$M = \begin{pmatrix} -a & 0 & c \\ a & -b & 0 \\ 0 & b & -c \end{pmatrix} \quad \text{(AM6)}$$

Then the differential equation is expressed as follows:

$$\boldsymbol{x}' = M\boldsymbol{x} \quad \text{(AM7)}$$

The general solution of this equation is given by the exponential function of a matrix (see Eq. (*AM*6)):

$$\boldsymbol{x}(t) = \exp(tM)\boldsymbol{C} = e^{tM}\boldsymbol{C} \quad \text{(AM8)}$$

where $\boldsymbol{C}$ a constant vector.

We define a domain Ω and the closure $\overline{\Omega}$ as follows:

$$\Omega = \{\boldsymbol{x} : x > 0, y > 0, z > 0\} \quad \text{(AM9)}$$

$$\overline{\Omega} = \{\boldsymbol{x} : x \geq 0, y \geq 0, z \geq 0\} \quad \text{(AM10)}$$

We further show that if a solution $\boldsymbol{x}(t)$ is in $\overline{\Omega}$ at $t = t_0$, then $\boldsymbol{x}(t)$ is in $\overline{\Omega}$ for all $t \geq t_0$. $\boldsymbol{x}(t) \equiv 0$ is a solution of the Eq. (*AM*8). Therefore, if a solution $\boldsymbol{x}(t)$ vanishes at some t_0, $\boldsymbol{x}(t_0) = 0$, then $\boldsymbol{x}(t) \equiv 0$ for all $t \geq t_0$.

When we assume as shown in the following equation,

$$x(t_0) > 0, y(t_0) = 0, z(t_0) = 0 \quad \text{(AM11)}$$

we obtain the statuses as shown in Eq. (*AM*12).

$$y'(t_0) = ax(t_0) > 0, z'(t_0) = 0, z''(t_0) = by'(t_0) = abx(t_0) > 0 \quad \text{(AM12)}$$

Thus, the following relation is obtained.

$$y(t) < 0 \text{for} t_0 - \varepsilon_1 < t < t_0 (\text{some} \varepsilon_1 > 0) \quad \text{(AM13)}$$

$$y(t) > 0, z(t) > 0 \text{for} t_0 < t < t_0 + \varepsilon_2 (\text{some} \varepsilon_2 > 0) \quad \text{(AM14)}$$

This shows that:

$$\boldsymbol{x}(t) \notin \Omega \text{for} t_0 - \varepsilon_1 < t < t_0 (\text{some} \varepsilon_1 > 0) \quad \text{(AM15)}$$

$$\boldsymbol{x}(t) \in \Omega \text{for} t_0 < t < t_0 + \varepsilon_2 (\text{some} \varepsilon_2 > 0) \quad \text{(AM16)}$$

When we assume as shown in the following equation,

$$x(t_0) > 0, y(t_0) > 0, z(t_0) = 0 \quad \text{(AM17)}$$

we obtain the statuses as shown in Eq. (*AM*18).

$$z'(t_0) = by(t_0) > 0 \quad \text{(AM18)}$$

Thus, the following statues are obtained.

$$z(t) < 0 \text{for} t_0 - \varepsilon_1 < t < t_0 (\text{some} \varepsilon_1 > 0) \quad \text{(AM19)}$$

$$z(t) > 0 \text{for} t_0 < t \leq t_0 + \varepsilon_2 (\text{some} \varepsilon_2 > 0) \quad \text{(AM20)}$$

This shows that:

$$\boldsymbol{x}(t) \notin \Omega \text{for} t_0 - \varepsilon_1 < t < t_0 (\text{some} \varepsilon_1 > 0) \quad \text{(AM21)}$$

$$\boldsymbol{x}(t) \in \Omega \text{for} t_0 < t < t_0 + \varepsilon_2 (\text{some} \varepsilon_1 > 0) \quad \text{(AM22)}$$

Appendix II-2: Differential equations: Characteristic function $\boldsymbol{f_M(t)}$ of the matrix $\boldsymbol{M}$

The characteristic function $f_M(t)$ of the matrix M is given as follows:

$$f_M(t) = \begin{vmatrix} t+a & 0 & -c \\ -a & t+b & 0 \\ 0 & -b & t+c \end{vmatrix} = t\left(t^2 + (a+b+c)t + (ab+bc+ca)\right) \tag{AM23}$$

Thus 0 is one of the eigen values of the matrix M (Eq. (*AM*6)). The discriminant D denotes the quadratic part of the characteristic function $f_M(t)$:

$$D = (a+b+c)^2 - 4(ab+bc+ca) \tag{AM24}$$

l and m denote the non-zero eigen values of the matrix M. Thus, we have the following status:

$$l + m = -(a+b+c) \tag{AM25}$$

$$lm = ab+bc+ca \tag{AM26}$$

Based on Eqs. (*AM*25) and (*AM*26) with $a > 0$, $b > 0$ and $c > 0$, the l and m are as follows.

$$l, m = \frac{-(a+b+c) \pm \sqrt{D}}{2} \tag{AM27}$$

The vectors $\boldsymbol{e}_l, \boldsymbol{e}_m, \boldsymbol{e}_0$ are respectively defined as shown in Eqs. (*AM*28), (*AM*29) and (*AM*30):

$$\boldsymbol{e}_l = \begin{pmatrix} (b+l)c \\ ac \\ (a+l)(b+l) \end{pmatrix} \tag{AM28}$$

$$\boldsymbol{e}_m = \begin{pmatrix} (b+m)c \\ ac \\ (a+m)(b+m) \end{pmatrix} \tag{AM29}$$

$$\boldsymbol{e}_0 = \begin{pmatrix} bc \\ ca \\ ab \end{pmatrix} \tag{AM30}$$

Then, vectors $\boldsymbol{e}_l, \boldsymbol{e}_m$ and $\boldsymbol{e}_0$ are eigen vectors corresponding to the eigen values l, m and 0. When $D < 0$, l and m are complex numbers conjugate to each other, and $\boldsymbol{e}_l$ and $\boldsymbol{e}_m$ are complex vectors conjugate to each other.

Appendix II-3

Appendix II-3-a: The case of $\boldsymbol{D} > 0$

In the case of $D > 0$, l and m are real (see Eq. (*AM*27)). Therefore, based on Eqs. (*AM*25) and (*AM*26), the following relations are obtained.

$$l + m = -(a+b+c) < 0 \tag{AM31}$$

$$lm = ab+bc+ca > 0 \tag{AM32}$$

Thus,

$$l < 0 \tag{AM33}$$

$$m < 0 \tag{AM34}$$

We define the matrix T as follows:

$$T = (\,\boldsymbol{e}_l \quad \boldsymbol{e}_m \quad \boldsymbol{e}_0\,) \tag{AM35}$$

Since each vector of the matrix T is an eigen vector, the following equation is obtained (see Eq. (*AM*6) regarding M):

$$MT = T\begin{pmatrix} l & 0 & 0 \\ 0 & m & 0 \\ 0 & 0 & 0 \end{pmatrix} \tag{AM36}$$

Therefore, the solution $\boldsymbol{x}(t)$ is given as follows:

$$\boldsymbol{x}(t) = e^{tM}\boldsymbol{C} = T\begin{pmatrix} e^{lt} & 0 & 0 \\ 0 & e^{mt} & 0 \\ 0 & 0 & 1 \end{pmatrix} T^{-1}\boldsymbol{C} \tag{AM37}$$

When C_1, C_2, C_3 are described as follows,

$$\begin{pmatrix} C_1 \\ C_2 \\ C_3 \end{pmatrix} = T^{-1}\boldsymbol{C} \tag{AM38}$$

the solution $\boldsymbol{x}(t)$ is given as follows:

$$\boldsymbol{x}(t) = e^{tM}\boldsymbol{C} = T\begin{pmatrix} C_1 e^{lt} \\ C_2 e^{mt} \\ C_3 \end{pmatrix} \tag{AM39}$$

Therefore, any component of the solution $\boldsymbol{x}(t)$ is described as a function of the following equation:

$$\varphi(t) = Ae^{lt} + Be^{mt} + C \tag{AM40}$$

Since $l < 0$ and $m < 0$ (see Eqs. (*AM*33) and (*AM*34)), there exists at most one t satisfying $\varphi'(t) = 0$. Namely each component of solution $\boldsymbol{x}(t)$ has at most one extremal value.

The matrix T defines a linear transformation of the (u, v, w)-space to the (x, y, z)-space. The above solutions in the (x, y, z)-space are the images of the following curves of the (u, v, w)-space by the linear transformation of T:

$$u = C_1 e^{lt} \tag{AM41}$$

$$v = C_2 e^{mt} \tag{AM42}$$

$$w = C_3 \tag{AM43}$$

Since $l < 0$ and $m < 0$ (see Eqs. (*AM*33) and (*AM*34)), (u, v) trends to$(0, 0)$ as $t \to \infty$.

Appendix II-3-b: The case of $\boldsymbol{D} < 0$

In the case where $D < 0$, the eigen values l and m are complex numbers conjugate to each other. We describe l and m as follows.

$$l = g + ih \tag{AM44}$$

$$m = g - ih \tag{AM45}$$

where $h > 0$. Then,

$$g = -\frac{a+b+c}{2} < 0 \tag{AM46}$$

Their eigen vectors $\boldsymbol{e}_l$ and $\boldsymbol{e}_m$ are complex vectors conjugate to each other. The real part and the imaginary part of $\boldsymbol{e}_l$ are respectively denoted by $\boldsymbol{p}$ and $\boldsymbol{q}$: That is,

$$\boldsymbol{p} = \begin{pmatrix} (b+g)c \\ ac \\ (a+g)(b+g) - h^2 \end{pmatrix} \tag{AM47}$$

$$\boldsymbol{q} = \begin{pmatrix} hc \\ 0 \\ (a+b+2g)h \end{pmatrix} \tag{AM48}$$

The matrix T is defined as follows:

$$T = (\,\boldsymbol{q} \quad \boldsymbol{p} \quad \boldsymbol{e}_0\,) \tag{AM49}$$

Then, the determinant $|T| = ac^2h(g^2 + h^2)$ of the matrix T is positive:

$$|T| = ac^2h\left(g^2 + h^2\right) > 0 \tag{AM50}$$

Thus, we obtain the flowing equations.

$$M\boldsymbol{q} = g\boldsymbol{q} + h\boldsymbol{p} \tag{AM51}$$

$$M\boldsymbol{p} = -h\boldsymbol{q} + g\boldsymbol{p} \tag{AM52}$$

$$MT = T\begin{pmatrix} g & -h & 0 \\ h & g & 0 \\ 0 & 0 & 0 \end{pmatrix} \tag{AM53}$$

When the matrix I and J are defined as Eqs. (*AM*54) and (*AM*55), the matrix R_θ of the rotation and a constant vector $\boldsymbol{c}$ are shown as Eqs. (*AM*56) and (*AM*57):

$$I = \begin{pmatrix} 1 & 0 \\ 0 & 1 \end{pmatrix} \tag{AM54}$$

$$J = \begin{pmatrix} 0 & -1 \\ 1 & 0 \end{pmatrix} \tag{AM55}$$

$$R_\theta = \begin{pmatrix} \cos\theta & -\sin\theta \\ \sin\theta & \cos\theta \end{pmatrix} \tag{AM56}$$

$$\boldsymbol{c} = \begin{pmatrix} C_1 \\ C_2 \end{pmatrix} \tag{AM57}$$

Then, we have Eq. (*AM*58).

$$MT = T\begin{pmatrix} g & -h & 0 \\ h & g & 0 \\ 0 & 0 & 0 \end{pmatrix} = T\begin{pmatrix} gI + hJ & 0 \\ 0 & 0 \end{pmatrix} \tag{AM58}$$

The following status holds:

$$\exp(tgI + thJ) = e^{gt}\begin{pmatrix} \cos(ht) & -\sin(ht) \\ \sin(ht) & \cos(ht) \end{pmatrix} = e^{gt}R_{(ht)} \tag{AM59}$$

Thus, we obtain the following equation.

$$\boldsymbol{x}(t) = e^{tM}\boldsymbol{C} = T\begin{pmatrix} e^{gt}R_{(ht)} & 0 \\ 0 & 1 \end{pmatrix}\begin{pmatrix} C_1 \\ C_2 \\ C_3 \end{pmatrix} = T\begin{pmatrix} e^{gt}R_{(ht)}\boldsymbol{c} \\ C_3 \end{pmatrix} \tag{AM60}$$

The matrix T defines a linear transformation of the (u, v, w)-space to the (x, y, z)-space. The above solutions in the (x, y, z)-space are the images of the following curves of the (u, v, w)-space by the linear transformation of T:

$$\begin{pmatrix} u \\ v \end{pmatrix} = e^{gt}R_{(ht)}\boldsymbol{c} \tag{AM61}$$

$$w = C_3 \tag{AM62}$$

Since$g < 0$, (u, v) tends to$(0, 0)$ as$t \to \infty$. Moreover, when the plane $w = C_3$ is viewed from a far positive point on the w-axis, the curve described by Eq. (*AM*61) runs counterclockwise. Since the determinant of the matrix $T$is positive (see Eq. (*AM*46)), and all components of the vector $\boldsymbol{e}_0$ are positive, all solutions run counterclockwise when we look at the plane $[k]$ from a far positive point on the z-axis.

Appendix II-4: Examples of $\boldsymbol{x}$, $\boldsymbol{y}$, $\boldsymbol{z}$

Appendix II-4-a: Example ($\boldsymbol{D} > 0$)

We deal with a case of

$$a = 0.15, b = 0.25, c = 1 \tag{AM63}$$

In this case, we have the following statuses:

$$D = 0.21, g = -0.7, l = -0.9291, m = -0.4709 \tag{AM64}$$

We define 20 different initial conditions as follows: for $k = 1, 2, \cdots, 20$.

$$C_1(k) = \cos\left(\frac{2\pi k}{20}\right) \tag{AM65}$$

$$C_2(k) = \sin\left(\frac{2\pi k}{20}\right) \tag{AM66}$$

$$C_3(k) = 3 \tag{AM67}$$

Then, we obtain the solutions $(u(t,k),\ v(t,k),\ w(t,k))$ with these initial conditions as follows:

$$u(t,k) = C_1(k)e^{lt} \tag{AM68}$$

$$v(t,k) = C_2(k)e^{mt} \tag{AM69}$$

$$w(t,k) = C_3(k) \tag{AM70}$$

The images $(x(t,k), y(t,k), z(t,k))$ using Eqs. (*AM*68), (*AM*69) and (*AM*70) with the linear transformation T (Eq. (*AM*35)) are given as follows:

$$x(t,k) = (b+l)cu(t,k) + (b+m)cv(t,k) + bcw(t,k) \tag{AM71}$$

$$y(t,k) = acu(t,k) + acv(t,k) + acw(t,k) \tag{AM72}$$

$$z(t,k) = (a+l)(b+l)u(t,k) + (a+m)(b+m)v(t,k) + abw(t,k) \tag{AM73}$$

Appendix II-4-b: Example ($\boldsymbol{D} < 0$)

We deal with a case of

$$a = 0.8, b = 0.9, c = 1 \tag{AM74}$$

In this case, we have the following statuses:

$$D = -2.39, g = -1.35, h = 0.7730 \tag{AM75}$$

We define the 8 different initial conditions as follows: for$k = 1, 2, \cdots, 8$.

$$C_1(k) = \cos\left(\frac{2\pi k}{8}\right) \tag{AM76}$$

$$C_2(k) = \sin\left(\frac{2\pi k}{8}\right) \tag{AM77}$$

$$C_3(k) = 3 \tag{AM78}$$

Then, we define the solutions $(u(t,k), v(t,k), w(t,k)$ with these initial conditions as follows:

$$u(t,k) = e^{gt}(C_1(k)\cos(ht) - C_2(k)\sin(ht)) \tag{AM79}$$

$$v(t,k) = e^{gt}(C_1(k)\sin(ht) + C_2(k)\cos(ht)) \tag{AM80}$$

$$w(t,k) = C_3(k) \tag{AM81}$$

The images $(x(t,k), y(t,k), z(t,k))$ of these $u(t,k),\ v(t,k),\ w(t,k)$ by the linear transformation T are respectively given as follows:

$$x(t,k) = hcu(t,k) + (b+g)cv(t,k) + bcw(t,k) \tag{AM82}$$

$$y(t,k) = acv(t,k) + acw(t,k) \tag{AM83}$$

$$z(t,k) = (a+b+2g)hu(t,k) + \left((a+g)(b+g) - h^2\right)v(t,k) + abw(t,k) \tag{A84}$$

References

[1] Marunaka R, Marunaka Y. Interactive actions of aldosterone and insulin on epithelial Na^+ channel trafficking. Int. J. Mol. Sci. 2020;21:3407. https://doi.org/10.3390/ijms21103407.

[2] Ilyaskin AV, Korbmacher C, Diakov A. Inhibition of the epithelial sodium channel (ENaC) by connexin 30 involves stimulation of clathrin-mediated endocytosis. J. Biol. Chem. 2021;296:100404. https://doi.org/10.1016/j.jbc.2021.100404.
[3] Ware AW, Rasulov SR, Cheung TT, Lott JS, McDonald FJ. Membrane trafficking pathways regulating the epithelial Na^+ channel. Am. J. Physiol. Renal Physiol. 2020;318(1):F1–F13. https://doi.org/10.1152/ajprenal.00277.2019.
[4] Marunaka Y. Characteristics and pharmacological regulation of epithelial Na^+ channel (ENaC) and epithelial Na^+ transport. J. Pharmacol. Sci. 2014;126(1):21–36. https://doi.org/10.1254/jphs.14R01SR.
[5] Marunaka Y, Marunaka R, Sun H, Yamamoto T, Kanamura N, Inui T, et al. Actions of quercetin, a polyphenol, on blood pressure. Molecules 2017;22(2):209. https://doi.org/10.3390/molecules22020209.
[6] Marunaka Y, Marunaka R, Sun H, Yamamoto T, Kanamura N, Taruno A. Na^+ homeostasis by epithelial Na^+ channel (ENaC) and Nax channel (Nax): cooperation of ENaC and Nax. Ann. Transl. Med. 2016;4(S1):S11.
[7] Marunaka Y, Niisato N, Miyazaki H, Nakajima K-I, Taruno A, Sun H, et al. Quercetin is a useful medicinal compound showing various actions including control of blood pressure, neurite elongation and epithelial ion transport. Curr. Med. Chem. 2019;25(37):4876–87.
[8] Marunaka Y. Actions of quercetin, a flavonoid, on ion transporters: its physiological roles. Ann. N. Y. Acad. Sci. 2017;1398:142–51. https://doi.org/10.1111/nyas.13361.
[9] Marunaka Y, Eaton DC. Effects of vasopressin and cAMP on single amiloride-blockable Na channels. Am. J. Physiol. Cell Physiol. 1991;260(5):C1071–84.
[10] Marunaka Y, Hagiwara N, Tohda H. Insulin activates single amiloride-blockable Na channels in a distal nephron cell line (A6). Am. J. Physiol. Renal Physiol. 1992;263(3):F392–400.
[11] Niisato N, Taruno A, Marunaka Y. Aldosterone-induced modification of osmoregulated ENaC trafficking. Biochem. Biophys. Res. Commun. 2007;361(1):162–8. https://doi.org/10.1016/j.bbrc.2007.07.002.
[12] Di Guglielmo GM, Drake PG, Baass PC, Authier F, Posner BI, Bergeron JJ. Insulin receptor internalization and signalling. Mol. Cell. Biochem. 1998;182:59–63.
[13] Kandror KV, Pilch PF. The sugar is sIRVed: sorting Glut4 and its fellow travelers. Traffic 2011;12:665–71. https://doi.org/10.1111/j.1600-0854.2011.01175.x.
[14] Laidlaw KME, Livingstone R, Al-Tobi M, Bryant NJ, Gould GW. SNARE phosphorylation: a control mechanism for insulin-stimulated glucose transport and other regulated exocytic events. Biochem. Soc. Trans. 2017;45:1271–7. https://doi.org/10.1042/bst20170202.
[15] Sasamoto K, Marunaka R, Niisato N, Sun H, Taruno A, Pezzotti G, et al. Analysis of aprotinin, a protease inhibitor, action on the trafficking of epithelial Na^+ Channels (ENaC) in renal epithelial cells using a mathematical model. Cell. Physiol. Biochem. 2017;41(5):1865–80. https://doi.org/10.1159/000471934.
[16] Marunaka R, Taruno A, Yamamoto T, Kanamura N, Marunaka Y. Action of protein tyrosine kinase inhibitors on the hypotonicity-stimulated trafficking kinetics of epithelial Na^+ channels (ENaC) in renal epithelial cells: analysis using a mathematical model. Cell. Physiol. Biochem. 2018;50:363–77. https://doi.org/10.1159/000494012.
[17] Marunaka R, Marunaka Y. Aldosterone action on epithelial Na^+ channel trafficking under the insulin-stimulated condition. J. Physiol. Sci. 2019;69:S252.
[18] Glynn E, Thompson B, Vadrevu S, Lu S, Kennedy RT, Ha J, et al. Chronic glucose exposure systematically shifts the oscillatory threshold of mouse islets: experimental evidence for an early intrinsic mechanism of compensation for hyperglycemia. Endocrinology 2016;157:611–23. https://doi.org/10.1210/en.2015-1563.
[19] Cherry EM, Hastings HM, Evans SJ. Dynamics of human atrial cell models: restitution, memory, and intracellular calcium dynamics in single cells. Prog. Biophys. Mol. Biol. 2008;98(1):24–37. https://doi.org/10.1016/j.pbiomolbio.2008.05.002.
[20] Li Y, Wang P, Xu J, Desir GV. Voltage-gated potassium channel Kv1.3 regulates GLUT4 trafficking to the plasma membrane via a Ca^{2+}-dependent mechanism. Am. J. Physiol. Cell Physiol. 2006;290(2):C345–51. https://doi.org/10.1152/ajpcell.00091.2005.
[21] Le Marchand SJ, Piston DW. Glucose suppression of glucagon secretion: metabolic and calcium responses from alpha-cells in intact mouse pancreatic islets. J. Biol. Chem. 2010;285(19):14389–98. https://doi.org/10.1074/jbc.M109.069195.
[22] Gao N, White P, Doliba N, Golson ML, Matschinsky FM, Kaestner KH. Foxa2 controls vesicle docking and insulin secretion in mature beta cells. Cell Metab. 2007;6:267–79. https://doi.org/10.1016/j.cmet.2007.08.015.
[23] Pouli AE, Emmanouilidou E, Zhao C, Wasmeier C, Hutton JC, Rutter GA. Secretory-granule dynamics visualized in vivo with a phogrin-green fluorescent protein chimaera. Biochem. J. 1998;333(Pt 1):193–9. https://doi.org/10.1042/bj3330193.
[24] Mikulovic S, Restrepo CE, Siwani S, Bauer P, Pupe S, Tort ABL, et al. Ventral hippocampal OLM cells control type 2 theta oscillations and response to predator odor. Nat. Commun. 2018;9(1). https://doi.org/10.1038/s41467-018-05907-w.
[25] Chen Y, Huang L, Qi X, Chen C. Insulin receptor trafficking: consequences for insulin sensitivity and diabetes. Int. J. Mol. Sci. 2019;20(20):5007. https://doi.org/10.3390/ijms20205007.
[26] Crudden C, Song D, Cismas S, Trocmé E, Pasca S, Calin GA, et al. Below the surface: IGF-1R therapeutic targeting and its endocytic journey. Cells 2019;8(10):1223. https://doi.org/10.3390/cells8101223.
[27] Kuremoto T, Kogiso H, Yasuda M, Inui T-A, Murakami K, Hirano S, et al. Spontaneous oscillation of the ciliary beat frequency regulated by release of Ca(2+) from intracellular stores in mouse nasal epithelia. Biochem. Biophys. Res. Commun. 2018;507(1-4):211–6. https://doi.org/10.1016/j.bbrc.2018.11.010.
[28] Yasuda M, Inui T-A, Hirano S, Asano S, Okazaki T, Inui T, et al. Intracellular Cl^- regulation of ciliary beating in ciliated human nasal epithelial cells: frequency and distance of ciliary beating observed by high-speed video microscopy. Int. J. Mol. Sci. 2020;21(11):4052. https://doi.org/10.3390/ijms21114052.
[29] Dee KU, Shuler ML. A mathematical model of the trafficking of acid-dependent enveloped viruses: application to the binding, uptake, and nuclear accumulation of baculovirus. Biotechnol. Bioeng. 1997;54:468–90. https://doi.org/10.1002/(sici)1097-0290(19970605)54:5<468::Aid-bit7>3.0.Co;2-c.
[30] García-Peñarrubia P, Gálvez JJ, Gálvez J. Spatio-temporal dependence of the signaling response in immune-receptor trafficking networks regulated by cell density: a theoretical model. PLoS One 2011;6. https://doi.org/10.1371/journal.pone.0021786.
[31] Khailaie S, Rowshanravan B, Robert PA, Waters E, Halliday N, Badillo Herrera JD, et al. Characterization of CTLA4 Trafficking and Implications for Its Function. Biophys. J. 2018;115(7):1330–43. https://doi.org/10.1016/j.bpj.2018.08.020.
[32] Stamper IJ, Wang X. Integrated multiscale mathematical modeling of insulin secretion reveals the role of islet network integrity for proper oscillatory glucose-dose response. J. Theor. Biol. 2019;475:1–24. https://doi.org/10.1016/j.jtbi.2019.05.007.